frontiers in Earth Science

ORIGINAL RESEARCH
published: 05 December 2019
doi: 10.3389/feart.2019.00312

Provenance and Sediment Maturity as Controls on CO_2 Mineral Sequestration Potential of the Gassum Formation in the Skagerrak

Mette Olivarius[1], Anja Sundal[2], Rikke Weibel[1], Ulrik Gregersen[1], Irfan Baig[2], Tonny B. Thomsen[1], Lars Kristensen[1], Helge Hellevang[2] and Lars Henrik Nielsen[1]*

[1] Geological Survey of Denmark and Greenland (GEUS), Copenhagen, Denmark, [2] Department of Geosciences, University of Oslo, Oslo, Norway

OPEN ACCESS

Edited by:
Amanda Owen, University of Glasgow, United Kingdom

Reviewed by:
Maria Ansine Jensen, The University Centre in Svalbard, Norway
Adrian John Hartley, University of Aberdeen, United Kingdom

***Correspondence:**
Mette Olivarius
mol@geus.dk

Specialty section:
This article was submitted to Sedimentology, Stratigraphy and Diagenesis, a section of the journal Frontiers in Earth Science

Received: *31 March 2019*
Accepted: *08 November 2019*
Published: *05 December 2019*

Citation:
Olivarius M, Sundal A, Weibel R, Gregersen U, Baig I, Thomsen TB, Kristensen L, Hellevang H and Nielsen LH (2019) Provenance and Sediment Maturity as Controls on CO_2 Mineral Sequestration Potential of the Gassum Formation in the Skagerrak. Front. Earth Sci. 7:312. doi: 10.3389/feart.2019.00312

In order to meet the increasing demand to decarbonize the atmosphere, storage of CO_2 in subsurface geological reservoirs is an effective measure. To maximize storage capacity, various types of saline aquifers should be considered including dynamic storage options with open or semi-open boundaries. In sloping aquifers, assessment of the immobilization potential for CO_2 through dissolution and mineralization along the flow path is a crucial part of risk evaluations. The Gassum Formation in the Skagerrak is considered a nearshore CO_2 storage option with sloping layers, facilitating buoyant migration of CO_2 northwards along depositional and structural dip. In this study, petrographic data and provenance analysis provide the basis for estimating reactivity of the sandstones. Immobilization of CO_2 in the reservoir through fluid dissolution and mineral reactions reduces risk of leakage. Petrographic analyses are integrated with seismic and well-log interpretation to identify sedimentary facies and to estimate mineral distribution with corresponding reactivity in the proposed injection area. Here the Gassum Formation comprises south-prograding, shoreface-fluvial para-sequences, sourced from northern hinterlands. Pronounced differences in the mineralogical maturity in the studied area are identified and explained by the sediment transport distances and the type of sediment source. This is possible because the U-Pb ages of zircon grains in the sediments can be used to pinpoint the areas where they originate from in the Fennoscandian Shield, such as the Telemarkia or Idefjorden terranes. Albite and Fe-rich chlorite are identified as the most reactive mineral phases in the Gassum sand, of which feldspar comprises the largest weight fraction and the grain-coating chlorite has largest surface area. Their distribution is partly controlled by provenance, so their abundance decreases basinwards with increasing sediment maturity. The abundance of fluvial sandstones presumably increases northwards in basal parts of para-sequences, while shoreface sandstones comprise the top part of sandy units. CO_2 injected in the proposed area will migrate upwards within the reservoir, toward higher proportions of Telemarkian-derived sediment and up-dip along the seal, toward more immature sediments. Thus, the reactivity of sediments increases

in younger deposits and up depositional dip, while kinetic reaction rates will decrease in shallower, lower temperature regions. Identifying these parameters is important to estimate the CO_2 mineral sequestration potential as a function of sedimentary facies and ensure safe storage of CO_2. This approach can advantageously be applied to all reservoirs considered for CO_2 injection to improve the estimation of the possible CO_2 storage volume by taking the provenance dependence of the mineralization potential into account.

Keywords: CO_2 storage, reactive minerals, source to sink, zircon geochronology, depositional environments, petrography, diagenesis, reservoir quality

INTRODUCTION

Subsurface, brine-saturated sandstone reservoirs hold great potential for safe storage of anthropogenic CO_2. Upscaling carbon capture and storage is recommended by the Intergovernmental Panel on Climate Change (IPCC) as means to meet goals of reducing greenhouse gas emissions (Metz et al., 2005). In Scandinavia, the offshore storage potential is huge (Halland et al., 2011; Bergmo et al., 2013; Anthonsen et al., 2014), but under-utilized with only two operating storage sites (Eiken et al., 2011). Thorough geological reservoir characterization is essential in risk evaluations where not only the reservoir volume and seal quality must be taken into account, but also the dissolution capacity and reactivity of the reservoir rocks such that the mineral sequestration potential can be estimated. Highly reactive minerals can ensure the largest amount of CO_2 carbonatization and the dependence of the mineral sequestration potential on the sediment provenance has largely been overlooked hitherto. The provenance and sediment transport may strongly influence the distribution of the most reactive minerals, which is investigated in this study.

The main objective in the Upslope project is to improve reservoir characterization schemes and optimize storage (Upslope, 2019). Coupled modeling is applied to estimate trapping efficiency and migration distances in the further adaptation of suitable injection schemes, ultimately ensuring safe storage in open-boundary, prospective reservoirs. In order to estimate CO_2 plume retardation and immobilization potential, knowledge of sedimentary facies distribution, with varying reservoir properties and reaction potentials, is essential. In particular, the modal mineralogical variations are of importance regarding the most reactive minerals with respect to carbonatization of CO_2 (Palandri and Kharaka, 2004).

The Gassum Formation has been thoroughly investigated throughout onshore Denmark due to its good reservoir quality that makes it applicable for geothermal energy exploitation (Nielsen, 2003; Kristensen et al., 2016; Weibel et al., 2017a). This knowledge can be utilized in the Skagerrak to evaluate prospective storage sites for CO_2. The reservoir properties of the Gassum Formation are not well known in the Norwegian sector, but it is evident that the pressure and temperature conditions are suitable for CO_2 storage. The Gassum Formation comprises fluvial to marginal marine sandy deposits interbedded with mudstones in the study area located at the northern rim of the Norwegian-Danish Basin in the Skagerrak (**Figure 1**; Hamberg and Nielsen, 2000; Nielsen, 2003). The formation constitutes a sloping aquifer in this area (**Figures 2**, **3**) that holds great potential for CO_2 storage (e.g., Halland et al., 2011; Bergmo et al., 2013; Anthonsen et al., 2014). There is a need, however, to constrain the mineralogical composition and reservoir quality to evaluate aspects of migration-assisted immobilization. In this respect, evidence of provenance areas and diagenetic evolution is required. A prospective injection site in the south-central part of the study area is assessed as an example (**Figure 1**).

Variations exist in the composition and sediment maturity of the Gassum Formation in the Norwegian-Danish Basin (Weibel et al., 2017a). This study investigates if regional maturity trends can be identified by comparing the sediments along the northern basin margin and in the Farsund Basin with those deposited centrally in the basin. The objective is to identify geographical and stratigraphical trends in sediment maturity related to the sediment transport distance and the lithology in the provenance terrane. If such relationships exist, then the modal mineralogical composition, and subsequently reactivity, can be estimated in potential CO_2 injection areas. New data of zircon ages and petrography provide improved understanding of provenance and diagenesis in the Gassum Formation aquifer on the Norwegian continental shelf, which can be applied in predictions of CO_2 carbonatization here and elsewhere.

GEOLOGICAL SETTING

The Upper Triassic to Lower Jurassic sandstone-dominated Gassum Formation is widely distributed in the Norwegian-Danish Basin and is, therefore, the favorite target for exploitation of geothermal energy onshore Denmark. The formation was first defined for the Danish area by Larsen (1966) and redefined as the upper part of the Mors Group by Bertelsen (1978, 1980). Deposition of the Gassum Formation took place in shoreface, estuarine, fluvial, lagoonal and lacustrine environments in the northern and eastern parts of the Norwegian-Danish Basin during the Rhaetian, while the contemporary shallow marine mudstones belonging to the Vinding Formation were deposited in the basin center. The facies change from the underlying continental red beds was accompanied by a shift to a more humid climate, which was probably already initiated in late Ladinian times. Marine mudstones of the Fjerritslev Formation

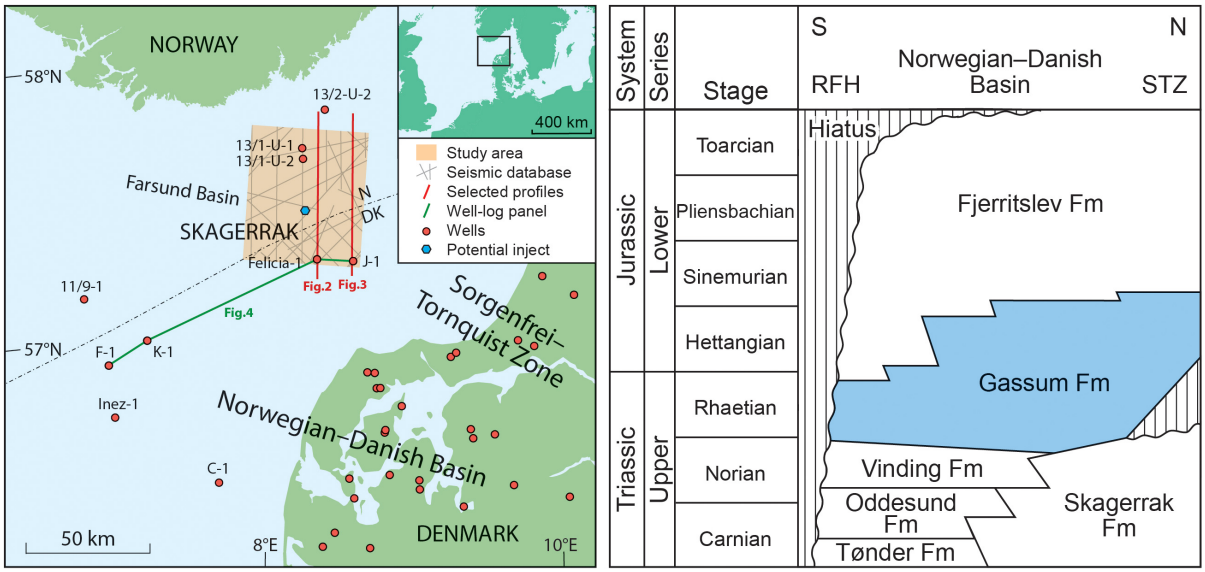

FIGURE 1 | The studied part of the Gassum Formation is located in the Skagerrak in the Norwegian-Danish Basin. The stratigraphic scheme depicts the basin from the Ringkøbing-Fyn High (RFH) to the Sorgenfrei-Tornquist Zone (STZ). The stratigraphy is based on Michelsen and Clausen (2002) and Nielsen (2003).

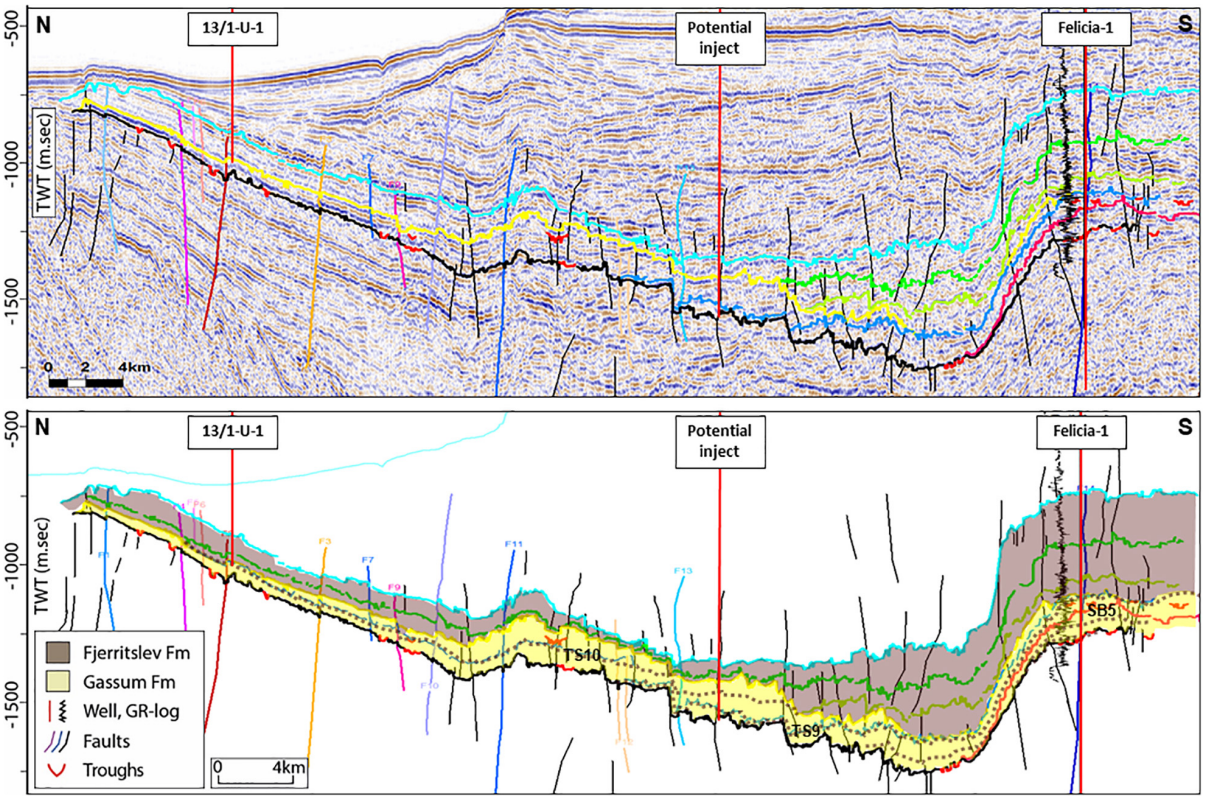

FIGURE 2 | Seismic profile from the Skagerrak showing that the Gassum Formation is sloping updip toward the north. The subtle troughs are possible channel structures. The 13/1-U-1 well and the potential injection site are projected (see **Figure 1**). The sequence boundary (SB5) and transgressive surfaces (TS9 and TS10) are interpreted in relation to the sequence stratigraphy by Nielsen (2003). The black faults are interpreted on this seismic profile only, whereas the colored faults tie between more seismic profiles. The northward onlapping internal seismic reflectors indicate that the lower part of the formation gradually disappears toward the basin margin.

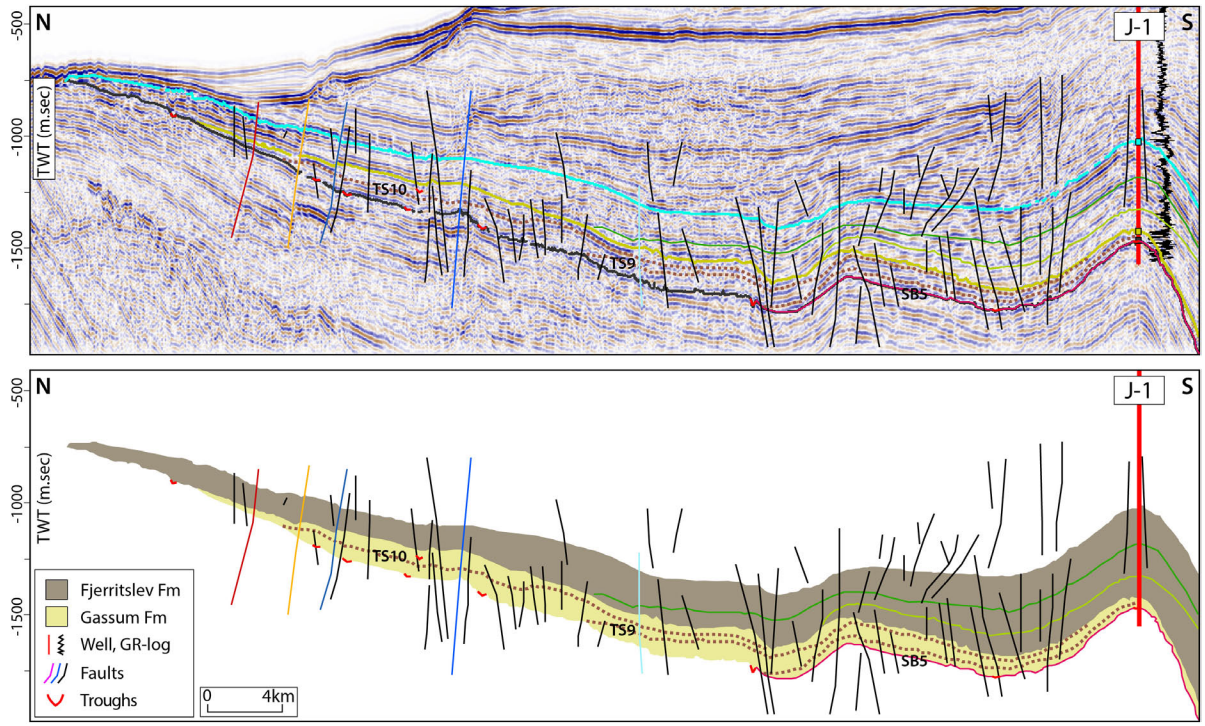

FIGURE 3 | Seismic profile from the Skagerrak located in the eastern part of the study area. The J-1 well is projected a short distance onto the profile (see **Figure 1**). See caption of **Figure 2** for further explanation.

were deposited during the early Jurassic while the deposition of sand moved northwards and the Gassum Formation was finally transgressed during the Early Sinemurian (Bertelsen, 1978, 1980; Michelsen, 1978; Hamberg and Nielsen, 2000; Nielsen, 2003; Lindström et al., 2009).

A Fennoscandian provenance of the Gassum Formation has been assumed based on the facies distribution in the basin (Bertelsen, 1980). The Fennoscandian Shield consists of an array of basement terranes formed at different times, which makes detrital zircon geochronology a powerful tool for interpreting the source areas of the sedimentary successions in the basin (Olivarius et al., 2014, 2017; Olivarius and Nielsen, 2016). The Paleozoic sediment cover in southwestern Sweden was removed during a middle Triassic uplift event and pronounced exhumation of southern Norway occurred during the Triassic where a succession of several kilometers thickness was eroded off (Rohrman et al., 1995; Japsen et al., 2016). Some Paleozoic sediments on the shield have been preserved such as in the Oslo Rift, but this is strictly local and it can be assumed that sediments constituted only a minor part of the exposed rocks of the Fennoscandian Shield during the Late Triassic.

The shield area positioned closest to the Skagerrak comprises the Sveconorwegian Orogen in southern Norway and Sweden, which consists of the Telemarkia Terrane, the Idefjorden Terrane and the Eastern Segment that formed at 1.52–1.48 Ga, 1.66–1.52 Ga, and 1.80–1.64 Ga, respectively (Bingen and Solli, 2009). Intrusions formed at 1.47–0.91 Ga and metamorphism occurred at 1.14–0.90 Ga in the Sveconorwegian belt and most pronouncedly in the Telemarkia Terrane (Bingen et al., 2008). The Idefjorden Terrane consists mostly of calc-alkaline plutonic and volcanic rocks and the Telemarkia Terrane is also primarily composed of plutonics and volcanics, where calc-alkaline signatures often are found in the felsic plutonic rocks (Brewer et al., 1998; Bingen et al., 2005). However, southeastern parts of the Telemarkia Terrane is a gneissic complex (Andersen et al., 2007). Clastic sediments formed in Pre-Sveconorwegian and early Sveconorwegian basins in both these terranes and they have mostly Sveconorwegian zircon ages, but also some older (Åhäll et al., 1998; Bingen and Solli, 2009). Magmatic zircon ages of 0.50–0.42 Ga are present in the Upper and Uppermost Allochthons in the Caledonian Orogen, whereas the Middle and Lower Allochthons have older ages of which most correspond to the basement windows in southern Norway of 1.69–1.62 Ga since these terranes are endemic to Fennoscandia (Bingen and Solli, 2009). Late Carboniferous to early Permian magmatism at 0.30–0.28 Ga caused extrusion of lavas in the Oslo Graben (Heeremans and Faleide, 2004).

MATERIALS AND METHODS

There are few wells and sparse core data available from the offshore parts of the Gassum Formation in the Skagerrak, especially from the Norwegian side. In the vicinity of the proposed storage area, only the well 13/1-U-1 was cored and

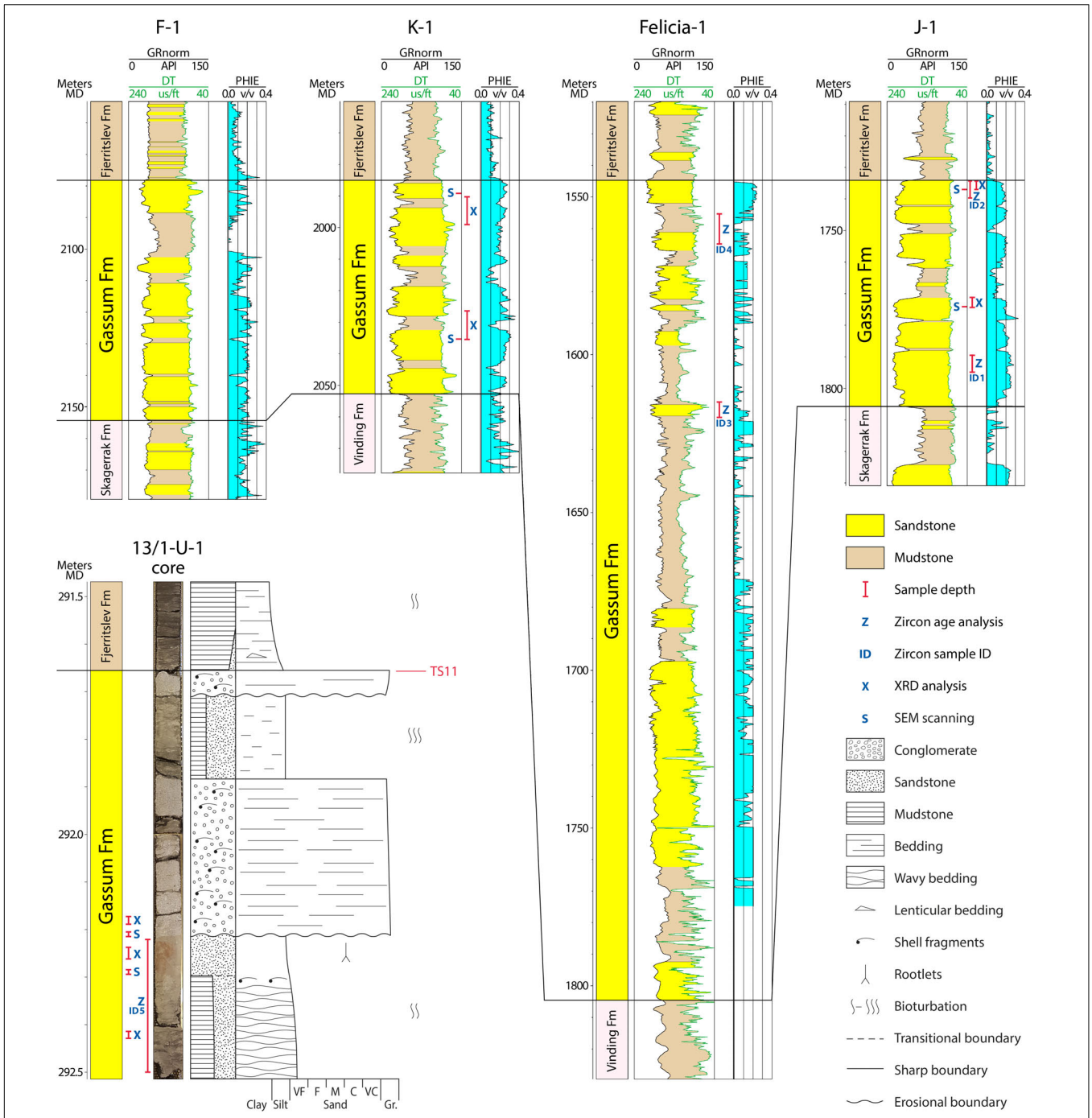

FIGURE 4 | Lithological columns of well-sections of the Gassum Formation with wireline logs and indicated sample depths. The lithostratigraphy is based on Nielsen and Japsen (1991). A sedimentological log of the cored section from the 13/1-U-1 well is shown alongside the core photos. Locations are shown in **Figure 1**. TS11 is a transgressive surface.

penetrates the top-most part of the Gassum Formation, as interpreted here (**Figures 2**, **4**). There is a continuous cored section through c. 170 m of the overlying Fjerritslev Formation and across the Gassum/Fjerritslev boundary. The nearest wells that have penetrated the Gassum Formation comprise the Felicia-1, J-1 and K-1 wells, from which only cuttings material and a few small sidewall cores are available. The reported depths are in meters below reference level (kelly bushing or rotary table).

Twelve samples were prepared as thin sections, including core from 13/1-U-1, cuttings from Felicia-1 and sidewall cores from J-1 and K-1. Seven samples were used for powder X-ray diffraction (XRD) analysis, including core from 13/1-U-1 and

cuttings from J-1 and K-1 (**Figure 4**). Five samples were selected for zircon age analysis comprising core from 13/1-U-1 and cuttings from Felicia-1 and J-1. The sample preparation requires up to 300 g of material to obtain a sufficient number of zircon grains, so a larger depth range was sampled than for the other types of analyses.

Polished thin sections were prepared with blue epoxy impregnation for easy porosity identification. The sidewall cores contained drilling mud with barite and mixed clays, and many grains in the samples were fractured during drilling, still, it was possible to characterize the rock texture. Grain-size distributions were obtained by measurements of minimum 100 grains. Grain size was determined according to the Wentworth scale (Wentworth, 1922) and sorting according to Folk (1966). Thin sections were studied by optical microscopy and scanning electron microscopy (SEM). Samples were carbon coated and examined at the University of Oslo SEM laboratory, using a Hitachi SU5000 FE-SEM (Schottky FEG) instrument including low-vacuum mode and in-lens SE-detector. Semi-quantification of mineralogy was performed as elemental analysis where the coloration is produced by mixing the colors of each element that is measured in each mineral.

The XRD analyses were performed on bulk samples of micronized sand and clay (Mc Crone mill) using a Bruker D8 Advance instrument applying CuKα radiation with Lynxeye detector and 90-position sample changer for high sample throughput. Bruker Eva software was used for phase identification (COD and PDF databases), and Profex BGMN for phase quantification applying Rietveld refinement. For core samples, the bulk mineral content estimated as weight percentage (wt.%) is representative contrary to sidewall core and cuttings samples where the clay, salt and sheet silicate contents are not representative due to contamination with drilling mud additives (e.g., gypsum, bentonite, barite). Thus, refinement results are normalized for the sand fraction as relative quartz/plagioclase (albite, oligoclase)/K-feldspar (intermediate microcline) contents.

Zircon U-Pb geochronological analyses were carried out at GEUS by laser ablation inductively coupled plasma mass spectrometry (LA-ICPMS), using a NWR 213 laser ablation instrument coupled to an Element2 magnetic sector-field ICPMS. The cuttings samples were first washed to remove drilling mud, then crushed and sieved to extract zircons from the 45–750 μm grain size fraction. The zircon grains were handpicked from heavy mineral concentrates obtained by density sorting using a Holman-Wilfley water-shaking table, and then embedded in epoxy, imaged by SEM at GEUS, and analyzed by LA-ICPMS. The zircons were ablated for 30 s in an air-tight helium-flushed chamber using a focused laser beam with a diameter of 25 μm, a repetition rate of 10 Hz and an output energy of ∼10 J/cm^2. The liberated material was transported through inert Tygon tubing by the helium carrier gas to the mass spectrometer for isotopic determination. To minimize instrumental drift, a standard-sample-standard analysis protocol was followed, bracketing the zircon analyses by measurement of the zircon standard GJ-1 (Jackson et al., 2004). For quality control, two secondary zircon standards were used, viz. Plešovice (Slama et al., 2008) and Harvard 91500 (Wiedenbeck et al., 1995, 2004), both yielding an average age accuracy and precision (2σ) within 3% deviation. Data reduction was performed using the Iolite software (Hellström et al., 2008; Paton et al., 2011; Petrus and Kamber, 2012). $^{207}Pb/^{206}Pb$ ages were used for zircons older than 700 million years (Ma), whereas $^{206}Pb/^{238}U$ ages were used for younger zircons, because the $^{206}Pb/^{238}U$ ages yield more robust ages and lower uncertainties (2σ) below 700 Ma. Common-lead correction was applied to a subset of the analyses when required, using measured mass 204 (i.e., $^{204}Hg + {}^{204}Pb$) corrected for Hg through the $^{202}Hg/^{204}Hg$ natural abundance ratio. Combined histogram and probability-density plots were produced through the software jAgeDisplay (Thomsen et al., 2016).

RESULTS

Sedimentology

In the Norwegian area, the Gassum Formation has only been drilled in the Farsund Basin by the 13/1-U-1 well, whereas the 13/1-U-2 and 13/2-U-2 wells did not reach the formation so no well logs exist from the northern part of the study area. The lowermost part of the 13/1-U-1 core is thus of great importance. Sedimentological investigation of the core with base at 292.52 m reveals that the lowermost 22 cm consists of heterolithic sand- and mudstone with wavy bedding and moderate bioturbation (**Figure 4**). Shell fragments occur near the top of the heterolith where there is a gradual transition to 9 cm of very fine-grained to silty sandstone displaying rootlets near the top. After an erosional boundary follows a 33 cm thick conglomerate with granule-sized clasts and abundant shell fragments. A sharp boundary marks the shift to the overlying 17 cm of sandstone-mudstone heterolith with abundant bioturbation, which is followed by an erosive boundary to the uppermost 5 cm of the formation that comprises a conglomerate with abundant shell fragments. The bivalve *Gryphaea Arcuata* (Lamarck) is identified in the core and is common in the Lower Sinemurian shallow-marginal marine deposits of southern Sweden (Troedsson, 1951). The lower c. 37 m of the overlying Fjerritslev Formation consists of an upward-coarsening para-sequence with beds of lenticular bedded silty mudstones, thin siltstones and very fine-grained sandstones that are moderate to intensely bioturbated. Based on the palynomorph assemblage, the succession is correlated to the Lower Sinemurian Bucklandi–Semicostatum zone (Smelror et al., 1989; Dybkjær, 2019, pers. comm.). A sharp boundary is present on top of this sequence after which a thick succession of stratified mudstones were deposited.

The combination of bioturbated, wavy bedded heteroliths, fine-grained sandstones with rootlets and conglomerates with shell debris suggest a vegetated paralic environment subjected to repeated flooding. The conglomerates with their erosive bases and high abundance of reworked shells are interpreted as lags formed during transgressive marine erosion. The boundary to the overlying deeper marine deposits is correlated to the transgressive surface TS 11, which occurs at the top of marine sandstones in parts of the basin and defines the top of the Gassum Formation

in more proximal located wells in the Fjerritslev Trough and on the Skagerrak-Kattegat Platform (Nielsen, 2003).

The seismic stratigraphic interpretation uses the sequence stratigraphic framework made by Nielsen (2003) for the Gassum Formation. The interpreted seismic lines in the study area are shown by their surface trace in **Figure 1**, and they tie to a regional grid that can be followed to the onshore part of the basin where more well data and cores exist. The internal seismic reflectors of the Gassum Formation in the study area include the regional mid-Rhaetian sequence boundary SB5 and the Hettangian transgressive surfaces TS9 and TS10. These surfaces show northward onlap, and the upper part of the Gassum Formation shows younging in the same direction (**Figures 2**, **3**) as also indicated by the Lower Sinemurian bivalves and palynomorphs found in the 13/1-U-1 core as described above, in contrast to the Hettangian age of the top of the Gassum Formation in J-1 identified by ostracods of the *O. aspinata* Zone (Michelsen, 1975). This conforms with the distal-proximal development seen elsewhere in the basin (Nielsen, 2003) and indicates that the lower part of the formation gradually pinches out toward the north and that the formation top is highly diachronous getting younger near the basin margin similar to what is observed in other parts of the basin (Nielsen, 2003; Weibel et al., 2017a). The identified seismic morphological troughs are possible channel systems (**Figure 5**), which suggest that fluvial deposits become more abundant toward the north in accordance with the overall sequence stratigraphic model. The interpretation focused on small U-shaped troughs, which were possibly not caused by faulting as seen by their position away from the faults, whereas apparent trough structures associated with faults have not been mapped since they may be caused by the faulting. The troughs occur where channels would be expected, which is along the base of sequence boundaries and para-sequences. A few of the troughs seem to coincide with the base of fluvial channels interpreted in Felicia-1 (**Figure 2**).

For the F-1, K-1, Felicia-1, and J-1 wells, the depositional environments have been interpreted based on well-log patterns, samples of cuttings and sidewall cores and palynological analyses since no conventional cores are available. The intercalated sandstone-mudstone succession in the upper part of the formation above SB5 has been interpreted as thin shoreface sandstones and marine mudstones formed in response to small sea-level fluctuations (**Figure 6**), which are also identified in other parts of the basin (Hamberg and Nielsen, 2000; Nielsen, 2003). The well-log pattern of a shoreface sandstone is typically sharp-based and blocky to funnel-shaped reflecting that it rests on a wave-scoured surface and consists of several thin sandstone units that may be almost amalgamated or separated by shoreface-offshore transition zone heteroliths. The thicker sandstone bodies near the base of the Gassum Formation in the F-1, Felicia-1, and J-1 wells display gamma-ray signatures that resemble estuarine sandstones as seen by their thick development and variable internal log pattern with bell- and funnel-shaped motifs due to the heterolithic component. The methodology for interpretation of facies associations from well-log patterns in the Gassum Formation is described in detail by Hamberg and Nielsen (2000) and Nielsen (2003), and the sequence stratigraphic surfaces are identified in accordance with Van Wagoner et al. (1990). The mid-Rhaetian sequence boundary SB5 occurring basin-wide in the Norwegian-Danish Basin typically cuts into marine mudstones. It is placed below estuarine deposits in F-1 and J-1 and it is traced to the base of thin shoreface deposits in K-1

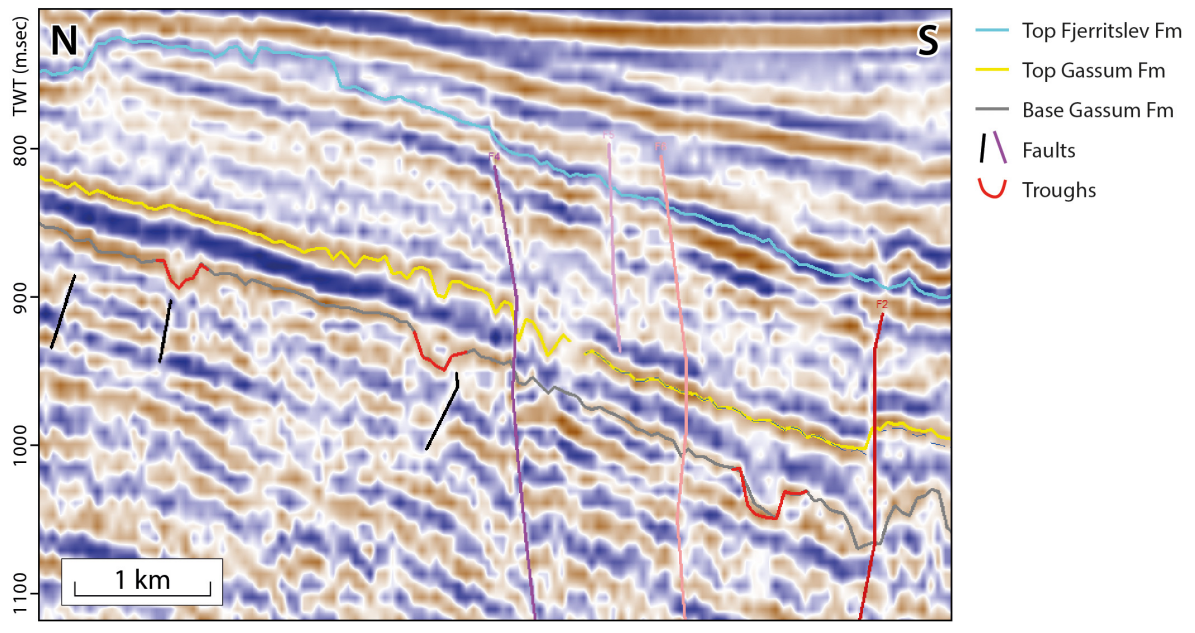

FIGURE 5 | Examples of seismic troughs, which are common in the study area and represent possible channel structures. The figure presents a close-up of the northern end of **Figure 2**.

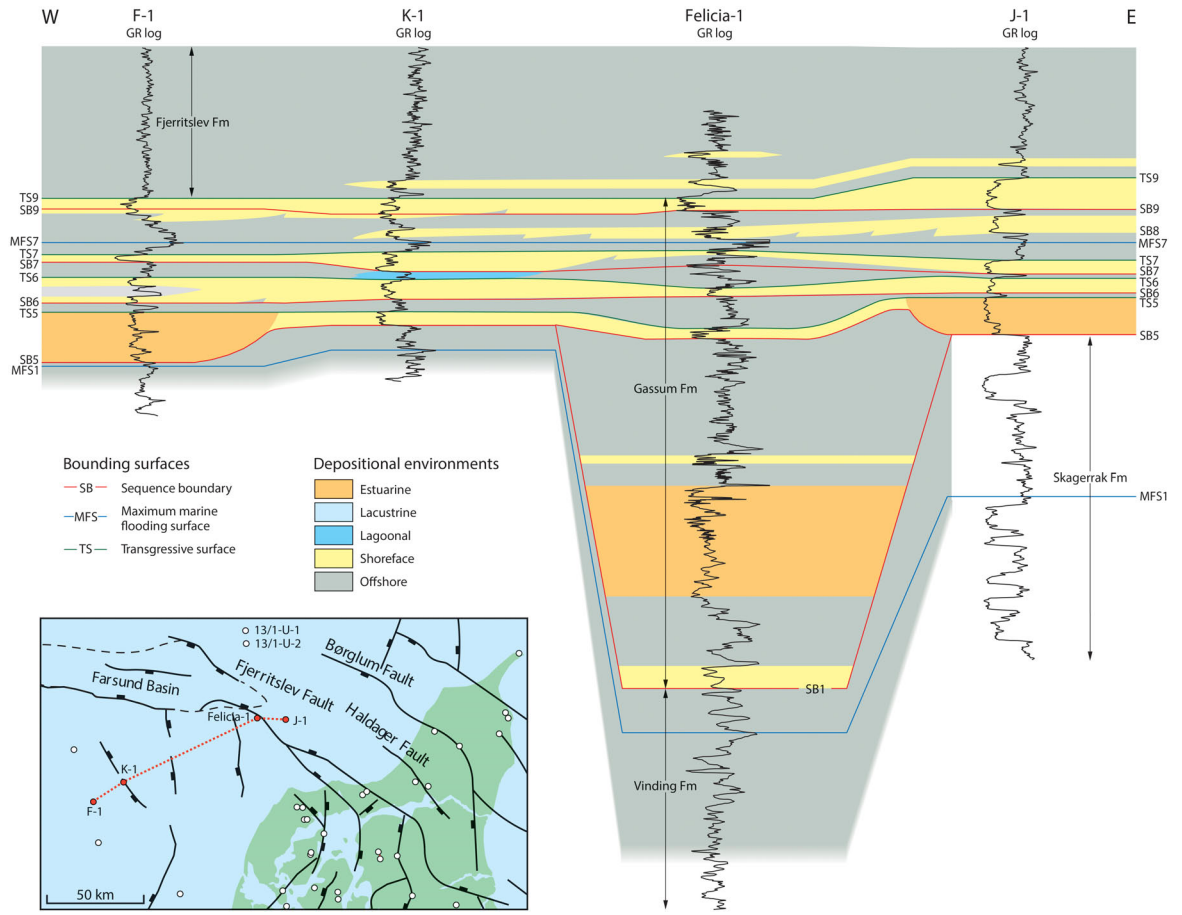

FIGURE 6 | Interpreted sequence stratigraphy and depositional environments of the Gassum Formation in the Skagerrak tied to the framework defined in wells onshore Denmark by Nielsen (2003). Oblique depositional dip section. The MWD-GR (measured while drilling – gamma ray) log is used for Felicia-1 since this is the most reliable because caving occurred during drilling.

and Felicia-1 (**Figure 6**). The overall pattern of the sequences of marine sandstones and mudstones overlying SB5 in the study area is backstepping in accordance with the general pattern in the basin with sequence boundaries marking the base of the sandstones and transgressive surfaces at their top. The latest Rhaetian basin-wide marine maximum flooding surface MFS7 is marked by claystones with extraordinarily high gamma-ray response (Nielsen, 2003).

The formation is much thicker in the Felicia-1 well compared to the three other wells in the area, which is interpreted as caused by deposition in the rim syncline of the closely located salt structure (Vejbæk and Britze, 1994). According to the seismic interpretation, the oldest part of the Gassum Formation below SB5 in the study area only occurs in the Felicia-1 area (**Figures 2**, **6**) since accommodation space was produced by the salt pillow forming to the southwest of the well, which caused the formation of a local basin. This lower part of the succession in Felicia-1 is not considered in this study since it is not present in the proposed injection area. In the 13/1-U-1 well, only the uppermost 86 cm of the Gassum Formation was penetrated, so the depositional facies in the deeper part are unknown, but fluvial deposits are likely to prevail in accordance with the general depositional pattern found in the basin (Nielsen, 2003) since the well is positioned more proximal to the Fennoscandian Shield than the other studied wells.

Based on these new findings, it was possible to construct a schematic north-south cross-section of the Gassum Formation from the Sorgenfrei-Tornquist Zone to the Norwegian-Danish Basin (**Figure 7**). The interpreted sequence-stratigraphic surfaces and depositional environments in J-1 are used as the southern end-point and the transgressive lag overlaying subaerial deposits in 13/1-U-1 comprises the northern end-point, where the proposed injection site is projected onto this schematic section (**Figures 4**, **6**). It is inferred that the predominance of shoreface sandstones in the central part of the basin is replaced by fluvial sandstones with fewer intercalated mudstones toward the basin margin. The marine mudstones are dominant toward the south, whereas lacustrine mudstones may be present between the fluvial sandstones to the north. The distal parts of the youngest shoreface sandstone layers in the study area passes laterally into time-equivalent marine mudstones that form part of the lower Fjerritslev Formation, which together with the

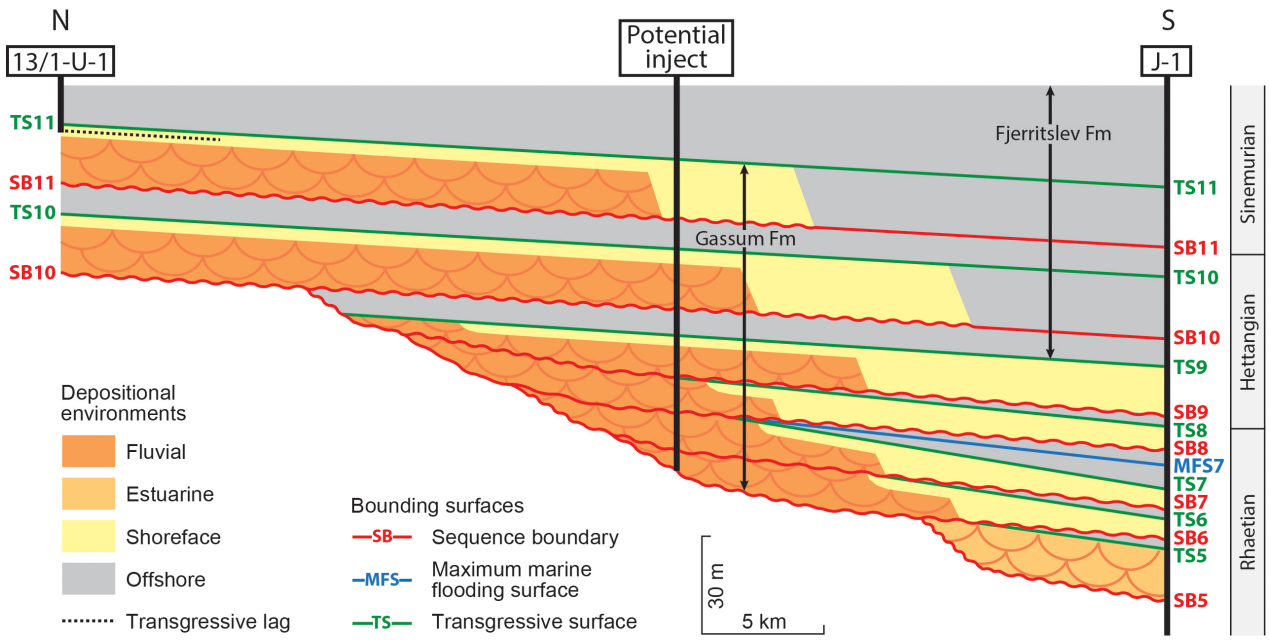

FIGURE 7 | Schematic north-south section from the Sorgenfrei-Tornquist Zone offshore Norway to the Norwegian-Danish Basin offshore Denmark. The sequence stratigraphic framework made by Nielsen (2003) is applied. The potential injection site is projected (see **Figure 1**).

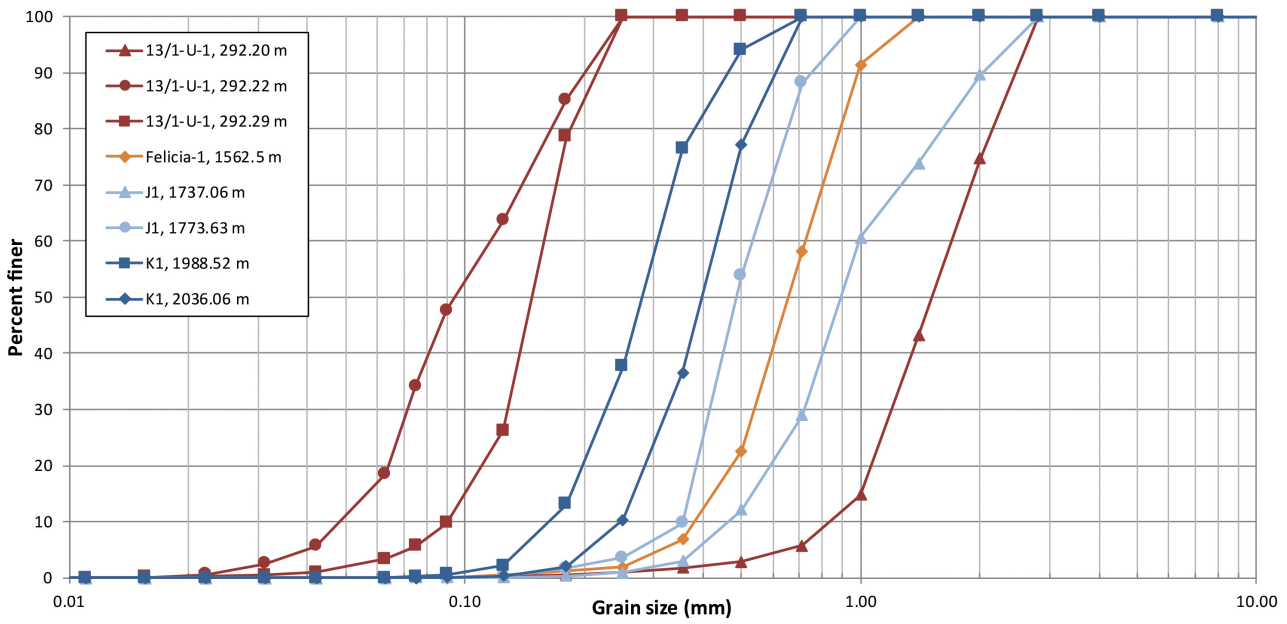

FIGURE 8 | Grain-size distributions of the Gassum Formation in the Skagerrak measured in thin sections.

northern onlap and pinch-out of the lower parts of the formation cause variations in the thickness of the Gassum Formation (**Figure 7**). These observations are in accordance with the consistent facies development that is documented in the onshore Danish area (Hamberg and Nielsen, 2000; Michelsen et al., 2003; Nielsen, 2003).

Petrography and Diagenesis

The studied sidewall core samples from the J-1 and K-1 wells and the cuttings sample from the Felicia-1 well represent a large spectrum of grain sizes ranging from fine- to very coarse-grained sandstones that are moderately to well sorted (**Figure 8**). Quartz is the dominant detrital component and feldspar consisting of

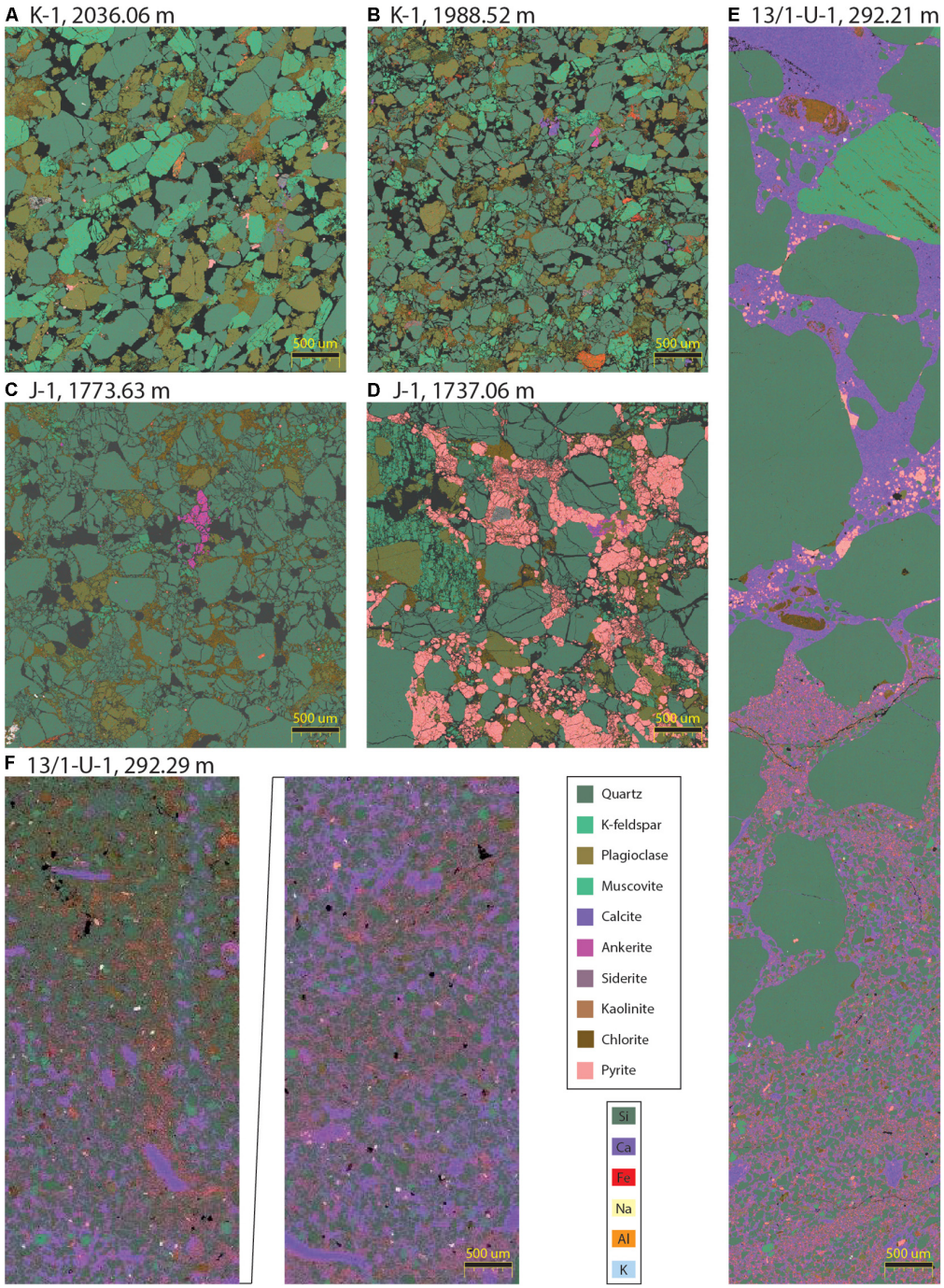

FIGURE 9 | Mineral semi-quantification by SEM element scanning. **(A–D)** Sandstones from sidewall cores from the K-1 and J-1 wells are dominated by quartz grains besides plagioclase/albite and K-feldspar grains, whereas authigenic phases occur in small amounts except for pyrite cement in D that may represent a local pyrite concretion. **(E)** The conglomerate in the 13/1-U-1 core contains clasts of quartz, feldspar, fossil fragments and chlorite ooids embedded in ankerite cement. **(F)** The lower sandstone in the 13/1-U-1 core is cemented by low-Fe calcite.

K-feldspar and plagioclase/albite is abundant in most samples (**Figure 9**). Quartz grains with undulatory extinction is a minor to common component, especially among the largest grains, and polycrystalline quartz grains occur. Mica minerals, heavy minerals and rock fragments are rare, except for the upper sample from J-1 in which rock fragments are common. Rare glauconite and organic matter are found in the samples from K-1. Most of the sandstones are porous (**Figures 9**, **10A**).

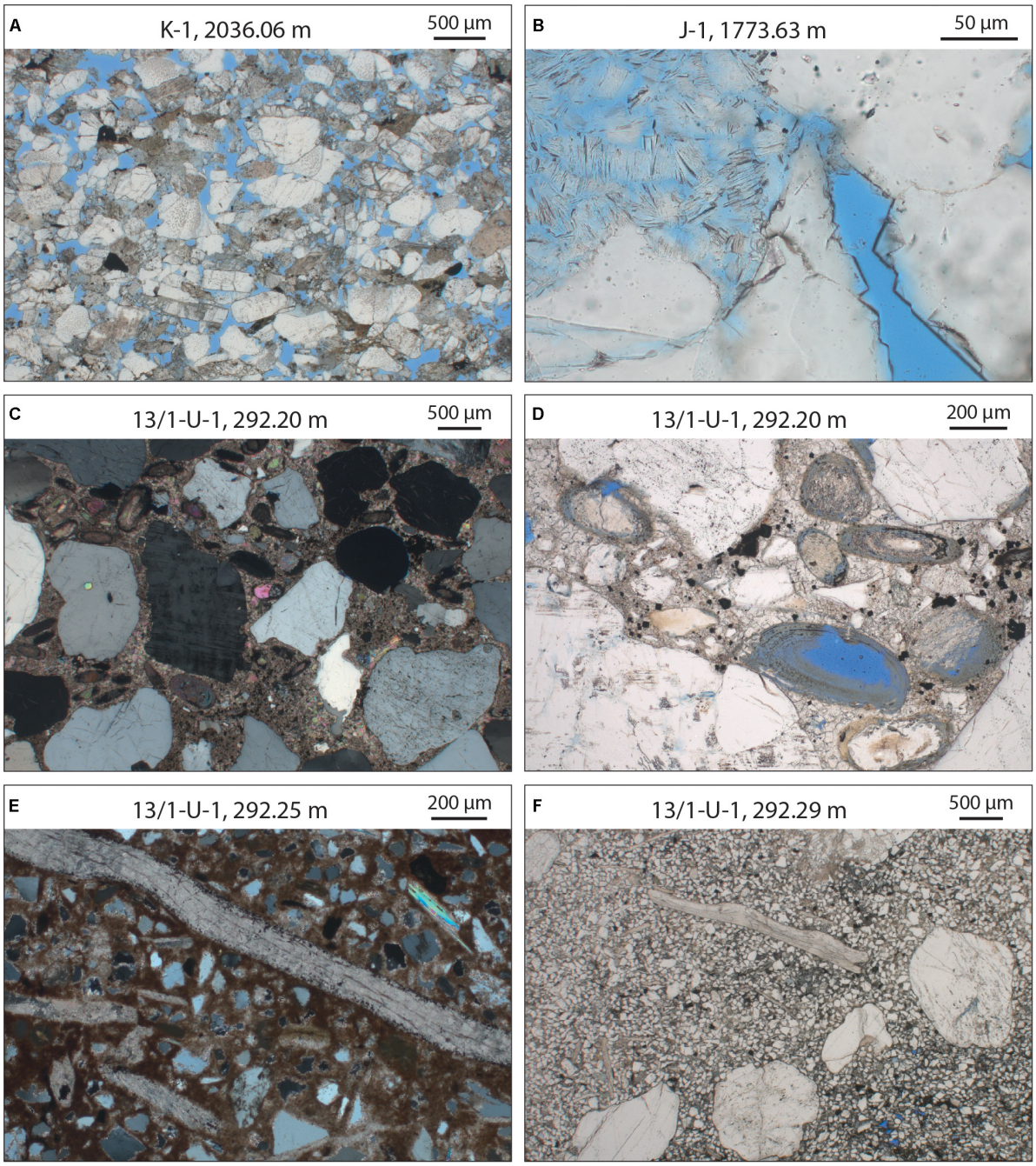

FIGURE 10 | Petrographic characteristics of the sampled sandstones. **(A)** Porous sandstone composed primarily of quartz and feldspar. **(B)** Thin quartz overgrowths enclosing kaolinite booklets. **(C)** Conglomerate with quartz and feldspar grains and chlorite ooids embedded in ankerite cement (crossed nicols). **(D)** Close-up of chlorite ooids. **(E)** Sandstone below the conglomerate with common shell fragments and siderite-ankerite cement (crossed nicols). **(F)** The lower part of the sandstone contains large grains dispersed in fine-grained sandstone with siderite-calcite cementation.

Thin quartz overgrowths is a recurrent authigenic phase and kaolinitic pore-fill is rare to common (**Figure 10B**). Minor to rare chlorite is found in most samples, sometimes as a patchy grain coating, and minor to rare illite has formed in the lower sample from K-1. Anatase and pyrite are minor to rare phases, except from the upper sample from J-1 that contains abundant pyrite cement (**Figure 9D**). Minor to common ankerite cement has formed in confined areas in the lower sample from J-1, where it has partly replaced some of the quartz grains and especially plagioclase and K-feldspar grains. K-feldspar overgrowths and albitization of microcline and oligoclase are occasionally observed. Some feldspar dissolution has occurred

in all samples and kaolinite booklets have formed in some of the secondary pores. Concerning the timing, anatase and pore-filling pyrite formed after kaolinite precipitation and feldspar dissolution. Anatase, pyrite and kaolinite formed prior to quartz overgrowths. The ankerite cement precipitated after some of the quartz cement and the quartz growth continued afterward.

The conglomerate in the 13/1-U-1 core (**Figure 4**) is studied in detail at its base at 292.21 m, where it is poorly sorted and contains grains and fossil fragments with lengths up to 5 mm (**Figure 9E**). The detrital components comprise primarily quartz and feldspar grains that are mostly 1–2 mm long, of which the quartz grains display rounded quartz overgrowths (**Figure 10C**). Many of the quartz grains have undulatory extinction, and plutonic rock fragments and polycrystalline quartz grains are present. The finer fraction contains also quartz and feldspar besides rare ilmenite, zircon, and abundant chlorite ooids that are 100–700 μm long. The ooids consist of a number of chamosite layers around nuclei of mica, quartz or feldspar that in most cases have been partly or fully replaced by ankerite (**Figure 10D**). The ooids were compacted prior to the pervasive ankerite cementation. The ankerite cement is sparry and has replaced fossil fragments and partly some detrital grains. Euhedral pyrite crystals are in some places abundant within the ankerite cement and tiny siderite rhombs and apatite crystals occur locally. Grain-coating chlorite occurs in some places and is thicker in embayments. Kaolinite has locally replaced grains, and secondary porosity has formed by partial dissolution of feldspar and the nuclei of ooids.

Quartz is the dominant detrital phase and feldspar is common in the moderately sorted, very fine-grained sandstone right beneath the erosional base of the conglomerate (**Figures 4**, **8**). Muscovite, chlorite and ilmenite grains and organic matter occur in minor amounts, whereas glauconite is minor to rare and zircon is rare. Shell fragments are common and up to 1 mm long and consists of low-Fe calcite (**Figure 10E**). Abundant siderite rhombs are dispersed in the pervasive ankerite cement, which has also formed within some of the dissolved nuclei of the rhombs. Tiny fragments of especially kaolinite, muscovite and quartz are present within the cement. Irregular chlorite coatings are found in some places and are thickest in embayments. Thin quartz overgrowths and albitization of K-feldspar is found locally. Further down, the sandstone becomes fine-grained and moderately well to well sorted (**Figure 8**), without considering the over-sized clasts of quartz and feldspar that are up to 2 mm long (**Figure 10F**). These large quartz grains have rounded overgrowths and some have undulatory extinction. Fossil fragments are common and consist of variating calcite and Fe-calcite. At 292.29 m, the pore-filling cement consists of low-Fe calcite (**Figure 9F**) with abundant siderite rhombs, framboidal pyrite and kaolinitic-illitic clay. Degraded biotite occurs in minor amounts and Fe-rich chlorite coatings occur locally. The heterolith at the base of the 13/1-U-1 core has a detrital composition that is comparable to the sandstone above but without carbonate cementation. Shell fragments are much less abundant and oversized clasts are not present. Some of the quartz grains have undulatory extinction.

TABLE 1 | Reservoir properties of the Gassum Formation based on well-log analysis.

Well	F-1	K-1	Felicia-1	J-1
Gross thickness	76 m	67 m	260 m	72 m
Net sandstone thickness	51 m	46 m	118 m	56 m
Net/Gross ratio	0.67	0.69	0.45	0.78
Porosity of sandstone	17–23%	20–28%	15–25%	18–25%

Reservoir Properties

The reservoir properties are estimated by well-log analysis where a porosity cutoff of 15% is used to define the sandstone intervals. For the F-1, K-1, and J-1 wells, the reservoir properties are comparable with a net sandstone thickness of 46–56 m, a net/gross ratio of 0.67–0.78 and a porosity range of 17–28% (**Table 1**). The much thicker succession encountered in the Felicia-1 well constitutes a special case with its net sandstone thickness of 118 m, net/gross ratio of 0.45 and porosity range of 15–25%. However, much caving occurred when the well was drilled, so the estimated reservoir properties of Felicia-1 may be subject to greater uncertainty than for the other wells. The available sidewall cores were not large enough for core analysis and the sandstones have become too crushed and deformed during drilling and sampling of the sidewall cores to make a reliable petrographic quantification of porosity.

Zircon Geochronology

The zircon age results are illustrated in **Figure 11** and the full dataset can be found in the online **Supplementary Table S1**. The zircon age distributions of the analyzed sandstones show that the sediment is derived from the Fennoscandian Shield where rocks with corresponding zircon ages are present, but some of their derived sediments may have been reworked prior to the deposition in the Skagerrak. Marked differences occur between some of the samples, showing that sediments were distributed differently in the basin during each of the depositional events. The zircon ages from the Gassum Formation are compared with published ages from the Fennoscandian Shield compiled by Bingen and Solli (2009).

The zircon age distribution of the lower sample from the J-1 well (Sample ID 1) has a broad age span with several age populations and associated prominent age peaks. The peak at 1.64 Ga corresponds to rocks included in the Caledonian Orogen domain and basement windows of central southern Norway, and the 1.49–1.48 Ga peak coincides with the formation of the Telemarkia Terrane in southernmost Norway. The younger Mesoproterozoic age peaks correspond to the magmatic and metamorphic ages associated with the Sveconorwegian Orogeny, which are far more abundant in the Telemarkia Terrane than in the Idefjorden Terrane and the Eastern Segment. Some of the zircons in the sample record ages that match the formation ages of the Idefjorden Terrane and the Eastern Segment. This is the only sample that contains zircon grains that record the Svecofennian Orogen/Transscandinavian Igneous Belt and the Oslo Graben areas, although these grains are few. Furthermore,

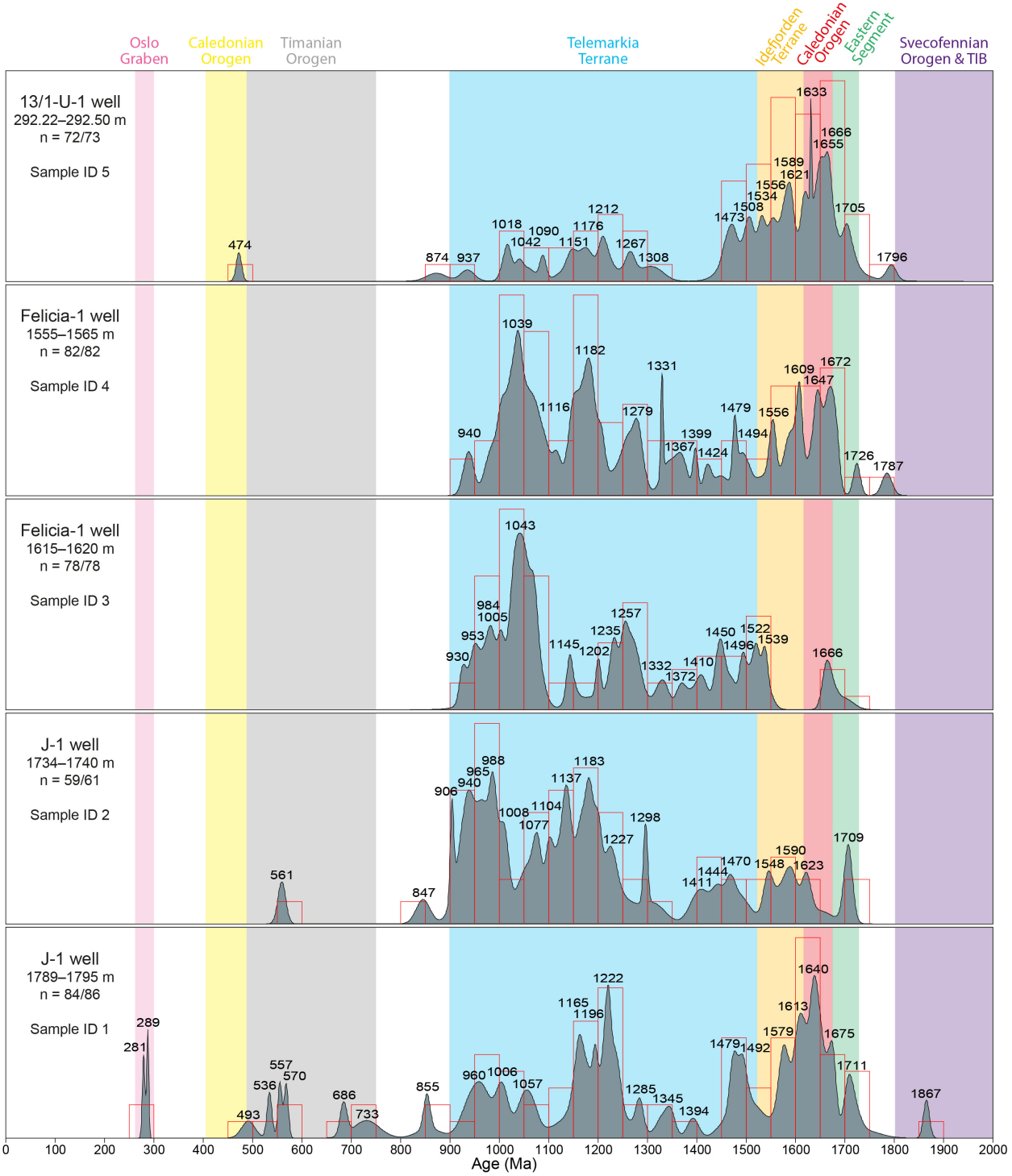

FIGURE 11 | U-Pb ages of zircon grains from the Gassum Formation in the Skagerrak plotted as probability density distributions and histograms. The number of employed concordant ages (discordance < 10%) out of the total number of measured ages is given by "n." See **Figure 4** for sampling positions in the wells and **Figure 12** for location of the wells and basement terranes.

this is the only sample with zircon ages that coincide with the age of the Timanian Orogen (c. 0.75–0.49 Ga) occurring far to the northeast. This orogen was eroded during the Cambrian-Ordovician and some of the produced detritus was deposited in southern Norway where it is outcropping in some areas (Slama, 2016).

The provenance of the three shoreface sandstones (Sample ID 2–4) is comparable and the zircon age distributions show that a large majority of the sediment is supplied from the Telemarkia Terrane in southernmost Norway, from which the Sveconorwegian ages are especially abundant in the samples. Some of the zircon ages also correspond to the Idefjorden Terrane, the Eastern Segment and the Caledonian Orogen domain including inherited ages and basement windows. Such zircons occur in small amounts in these sandstones and are most abundant in the upper sample from the Felicia-1 well (Sample ID 4). A single zircon grain with an age that matches the Timanian Orogen is found in the upper samples from the J-1 well (Sample ID 2).

The zircon age distribution of the sample from the 13/1-U-1 well (Sample ID 5) has its three most prominent age peaks at 1.67–1.63 Ga corresponding to ages in the middle and lower Caledonian allochthons and in basement windows in the Caledonian Orogen domain. Ages comparable to the Idefjorden Terrane and the Telemarkia Terrane are also common in the sample. This is the only sample where a zircon grain with age matching the timing of the Caledonian Orogen is found (0.47 Ga).

DISCUSSION

Provenance Signals

The interpreted source areas based on zircon ages from the Gassum Formation are shown in three scenarios in **Figure 12**. The lowstand scenario is based on the estuarine sandstone from J-1, whereas the highstand scenario merges the three shoreface sandstones from J-1 and Felicia-1 since they are of comparable provenance, and the transgressive scenario is based on the sandstone sample from 13/1-U-1. The thickness of the arrows indicates relative amounts of sediment supplied from each area. However, uncertainties are associated with this estimate, such as the variations in zircon fertility in the source areas and the hydraulic sorting occurring during transport (e.g., Malusà et al., 2016). Furthermore, the possibilities of reworking of older sediments and contamination of cuttings samples must be considered.

In the underlying Lower to Upper Triassic Skagerrak Formation, input from reworked Paleozoic sediments is observed in the Lower Triassic part of the formation where Caledonian zircon grains indicate a supply of reworked Silurian–Devonian sediments whereas this is not found in the upper part of the formation (Olivarius and Nielsen, 2016). This means that the deep erosion that occurred in southern Norway and southwestern Sweden during the Triassic has probably removed the majority of the Paleozoic sediment cover prior to the deposition of the Gassum Formation (Rohrman et al., 1995; Japsen et al., 2016).

The possibility of contamination of the cuttings samples from Felicia-1 and J-1 by cavings from younger deposits must be considered. For Felicia-1, it is known that caving occurred during drilling, whereas the caliper log from J-1 indicates a minimal amount of caving. The overlying Fjerritslev Formation is thickly developed in these areas (**Figures 2**, **3**) and presumably too fine-grained to contain zircons of sufficient size for U-Pb analysis, so cavings from this formation may not induce bias to the analyzed zircon age distributions. This assumption is based on knowledge of the Fjerritslev Formation, which consists mostly of claystone and contains siltstone laminae in some intervals besides few very fine-grained sandstones (Schmidt, 1985; Michelsen et al., 2003). The smallest zircon grains of less than 45 μm were sieved out of the samples prior to the U-Pb analyses so part of the possible silt-sized contamination would have been removed by this method. The possibly remaining contamination with coarse silt and very fine sand is assumed not to contain zircons since the settling equivalence that exists between light and heavy mineral grains means that the zircon grains in a sediment are smaller than the quartz grains (Garzanti et al., 2008). Furthermore, most of the zircons that have been extracted from the sediments are sand-sized (**Supplementary Figure S1**). The consistent provenance signal found in the zircon grains from the three shoreface sandstones is significantly different from the estuarine provenance signal from the fourth cuttings sample, which also indicates that cuttings contamination has not caused a significant artificial modification of the provenance signal. The most coarse-grained intervals of the Fjerritslev Formation have been deposited at the lower shoreface and therefore presumably have quite similar provenance signature as the shoreface sandstones in the upper part of the Gassum Formation, meaning that a zircon contamination would probably not even have changed the provenance signal much.

The provenance area of the estuarine sandstone (Sample ID 1) is rather large since the zircon grains originate from both southernmost Norway, central southern Norway and southwestern Sweden (**Figures 11**, **12**). This is the only sample with zircon ages matching the Svecofennian Orogen, the Timanian Orogen and the Oslo Graben, which shows that the source area is larger for this sample than for the remaining samples. The results indicate that the closer positioned sediment source areas supplied more sediment than the more distant source areas. This may be inferred from the larger amount of zircon ages matching the Telemarkia Terrane than the more northern Caledonian Orogen and from the progressively lower amount of zircon ages that correspond to the Idefjorden Terrane, the Eastern Segment and the Svecofennian Orogen, respectively. This may be because these three terranes are located progressively further away toward the northeast. Only a few ages coincide with the age of the Oslo Graben, which is probably because the zircon fertility is low in these extrusive rocks (Corfu et al., 2015). Timanian ages have not been encountered elsewhere in the Norwegian-Danish Basin (Olivarius and Nielsen, 2016), and such ages are rare in Fennoscandia since they correspond to the Timanian Orogen far to the northeast, which was eroded in Cambrian-Ordovician time where sediment was transported toward the southwest (Slama, 2016). These sediments are preserved locally in southern Norway, so it is likely that they have supplied detritus to proximal parts of the Gassum Formation in the study area. The reworking of such sediments would have increased the mineralogical maturity as observed for this sample.

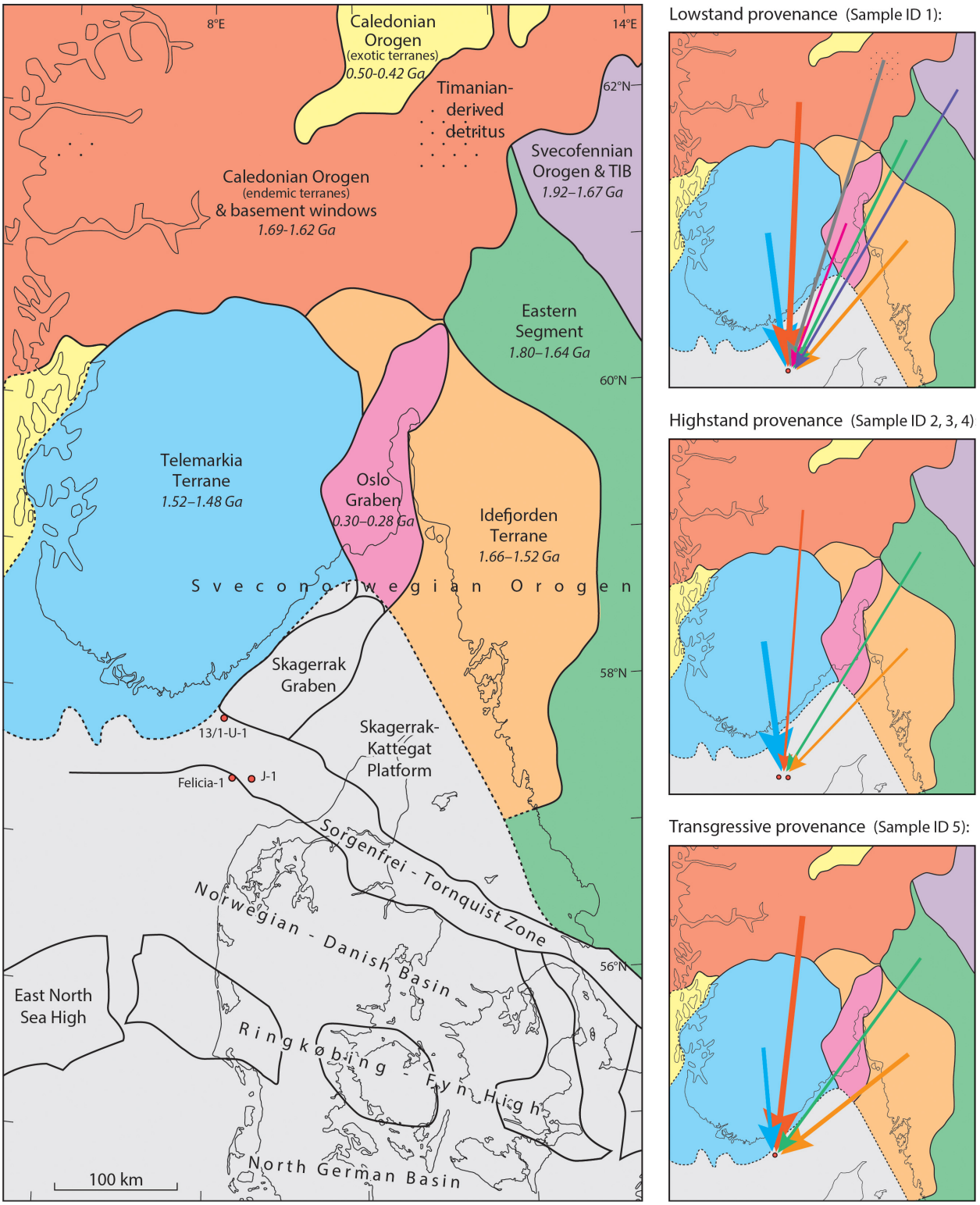

FIGURE 12 | Structural configuration of southern Scandinavia with the area of Triassic deposition shown in gray and indication of magmatic zircon ages of the major basement provinces in billion years (Ga). The map is based on Nielsen (2003), Heeremans and Faleide (2004), Lahtinen et al. (2008), Bingen and Solli (2009), Erlström and Sivhed (2012), Jarsve et al. (2014), and Slama (2016). The provenance interpretations are shown on the miniature maps where the thickness of the arrows is an indicator of the relative amount of sediment supplied from each terrane.

The prominent Telemarkian zircon age population found in all the shoreface sandstones (Sample ID 2–4) imply that the sediment was supplied almost exclusively from the southernmost Norway, which reveals a short transport distance from source to sink for most of the sediment. This is in accordance with the mineralogical immaturity of the sandstone in the sidewall core from the J-1 well at 1737.06 m, which corresponds to the upper zircon age sample from this well (Sample ID 2). Although the shoreface and transgressive samples (Sample ID 2–5) have quite similar age span, the relative proportion between the age populations is distinctly different, where the Telemarkian ages dominate the shoreface sandstones (Sample ID 2–4) and Caledonian and Idefjorden ages are dominant in the transgressive sandstone (Sample ID 5).

It is not surprising that young zircon ages corresponding to the timing of the Caledonian Orogeny are almost absent in the samples since only a limited amount of zircons was formed during this event. However, the inherited Paleoproterozoic zircon ages in the Caledonian Orogen are abundant in the estuarine and transgressive samples (Sample ID 1 and 5) indicating that favorable conditions for supplying sediment from central southern Norway to this part of the basin were present in these depositional environments. In the transgressive lag, reworking of the mineralogically immature sediments is a likely source of some of the deposited sediment as indicated by the content of coarse-grained quartz and feldspar grains in a very fine-grained matrix, and the quartz grains have rounded quartz overgrowths indicative of reworking of previous sandstones.

Temperature Indicators

The petrographic observations and reservoir properties extracted from the limited amount of samples and well logs that are available from the study area are in accordance with the detailed knowledge obtained for the Gassum Formation in the onshore Danish area (Kristensen et al., 2016; Weibel et al., 2017a,b). The new results are considered valid, but they represent individual examples of the reservoir and do not express the full variation that occur within the formation. Therefore, the average reservoir data from the onshore part of the formation are given in **Figure 13** to show the general characteristics of the depositional environments at different burial depths, and these results are assumed to concur with the sediment in the study area, except for the differences related to decreasing sediment maturity when approaching the source areas.

The petrographic relationships in the study area indicate that kaolinite has precipitated early during burial, which is in accordance with interaction with flowing meteoric water for its formation, and it sets limits on the maximum burial temperature since kaolinite is unstable at temperatures above c. 130°C when K-feldspar is present (Bjørlykke et al., 1986; Bjørlykke, 1998). Siderite normally precipitates early during burial (Morad, 1990; Hervig et al., 1995; Weibel et al., 2017b) and the presence of siderite means that the sandstones presumably not have been buried deeper than c. 3 km (c. 100°C). This is evident by the decreasing amount of siderite in the Gassum Formation onshore Denmark with increasing depth and its disappearance at a maximum burial depth of c. 3 km (Weibel et al., 2017b).

The thin macroquartz overgrowths signify that the sandstones were subjected to temperatures of c. 80–100°C since the onset of macroquartz formation normally occurs in this range, whereas it becomes extensive at higher temperatures (Bjørlykke et al., 2009; Weibel et al., 2010). The petrographic relationship between quartz overgrowths and ankerite cement shows that ankerite began precipitating after quartz, which is also observed in the Gassum Formation onshore Denmark (**Figure 13**), where it corresponds to a maximum burial depth of at least c. 2 km (c. 70°C). This is in accordance with other studies showing that the formation of ankerite normally requires temperatures of at least 75–80°C (Fisher and Land, 1986; Burley et al., 1989). The incipient albitization of some of the K-feldspar grains indicates that the sandstones have been exposed to temperatures of at least c. 65°C and not above c. 130°C where the albitization process would be almost complete (Bjørlykke et al., 1986; Saigal et al., 1988; Aagaard et al., 1990).

In conclusion, the diagenetic alterations observed in the sandstones give a consistent picture of the burial history and show that the Gassum Formation in the Skagerrak was subjected to maximum burial temperatures of c. 80–100°C corresponding to maximum burial depths of c. 2.3–3.0 km prior to structural inversion. This is in accordance with the thickness of the succession removed by Cenozoic exhumation that has been estimated by basin modeling based on sonic data to be 800 m for the Felicia-1 and J-1 wells and 600 m for the K-1 well (Japsen and Bidstrup, 1999; Japsen et al., 2007; Baig et al., 2019).

Reservoir Quality

The lack of core material makes it impossible to directly measure the porosity and permeability of the sandstones in the proposed injection area. However, the observed diagenetic development corresponding to maximum burial depths of c. 2.3–3.0 km can be used to compare the studied sandstones in nearby wells in the Skagerrak with their onshore equivalents where the Gassum Formation has been studied in detail based on core material from Danish wells. The results show that sandstones having been buried to this depth interval have average porosities of 22–32% and average gas permeabilities of 112–2757 mD, depending on their depositional environment (**Figure 13**). This porosity interval is higher than the porosities of 15-25% interpreted from Felicia-1 and J-1 well-logs (**Table 1**). However, both approaches give porosities that are sufficiently high for CO_2 injection. According to the applied sequence stratigraphic model, supported by the detailed seismic interpretation, the formation contains progressively more fluvial sandstones and less shoreface sandstones northwards across the Skagerrak (**Figure 7**). According to observations from the onshore facies, this would result in higher permeability due to both larger grain size and less cementation (Kristensen et al., 2016; Weibel et al., 2017a). This is in accordance with the medium to very coarse grain-size of the sandstones encountered in

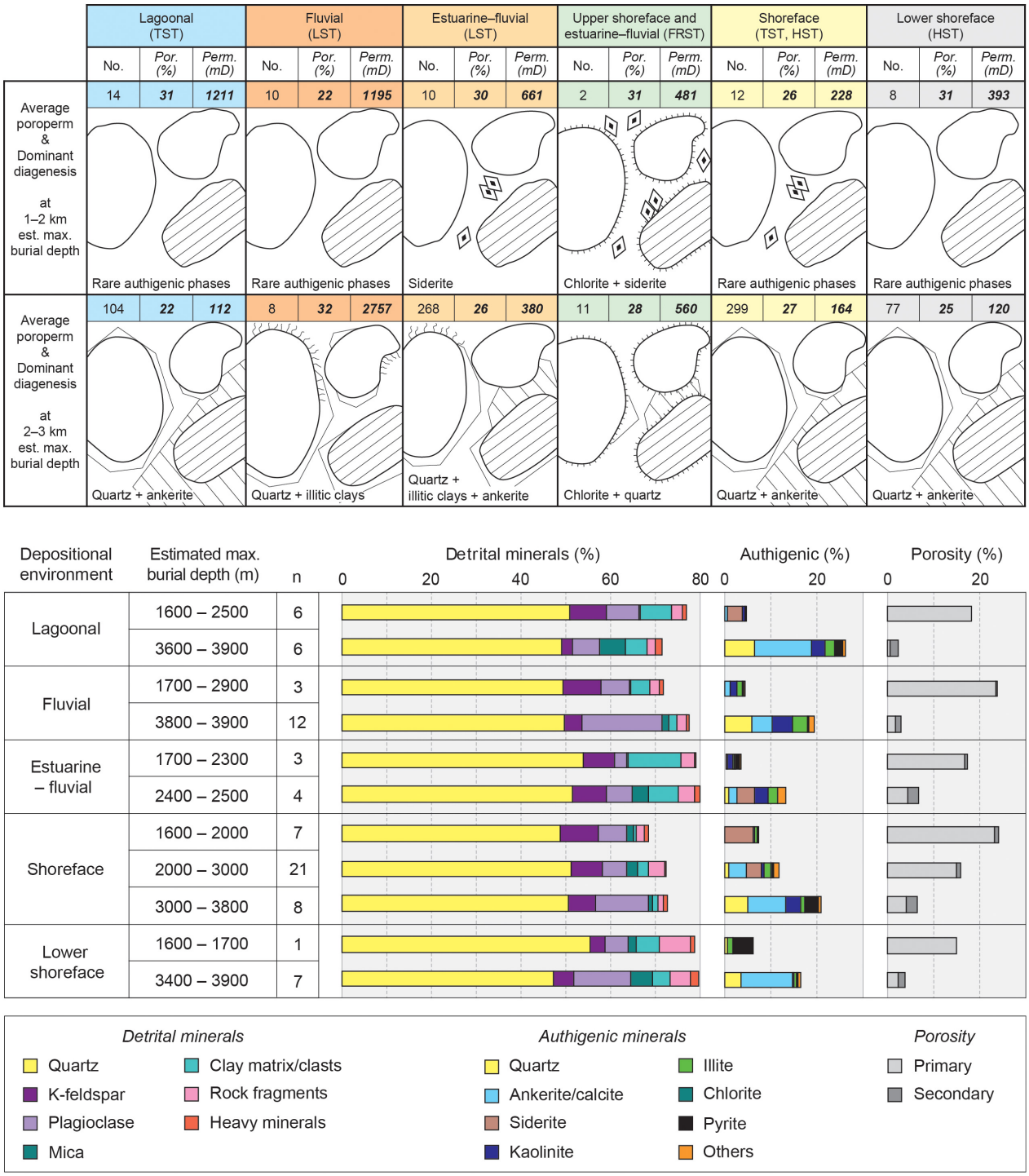

FIGURE 13 | Overview of the typical diagenetic alterations occurring in the different depositional environments and the resulting average porosity and permeability for estimated maximum burial depths of sandstones from the Gassum Formation onshore Denmark. The mineralogy is quantified by petrographic point counting. Modified from Weibel et al. (2017a). TST, transgressive systems tract; LST, lowstand systems tract; FRST, forced regressive systems tract; HST, highstand systems tract.

Felicia-1 and J-1 (**Figure 8**), whereas fine-grained sandstones are most abundant onshore Denmark followed by medium-grained sandstones while coarse-grained sandstones are rare (Weibel et al., 2017a). It is thus assumed that the net/gross ratio increases northwards due to deposition of less marine mud and more local sand, so all points toward that the

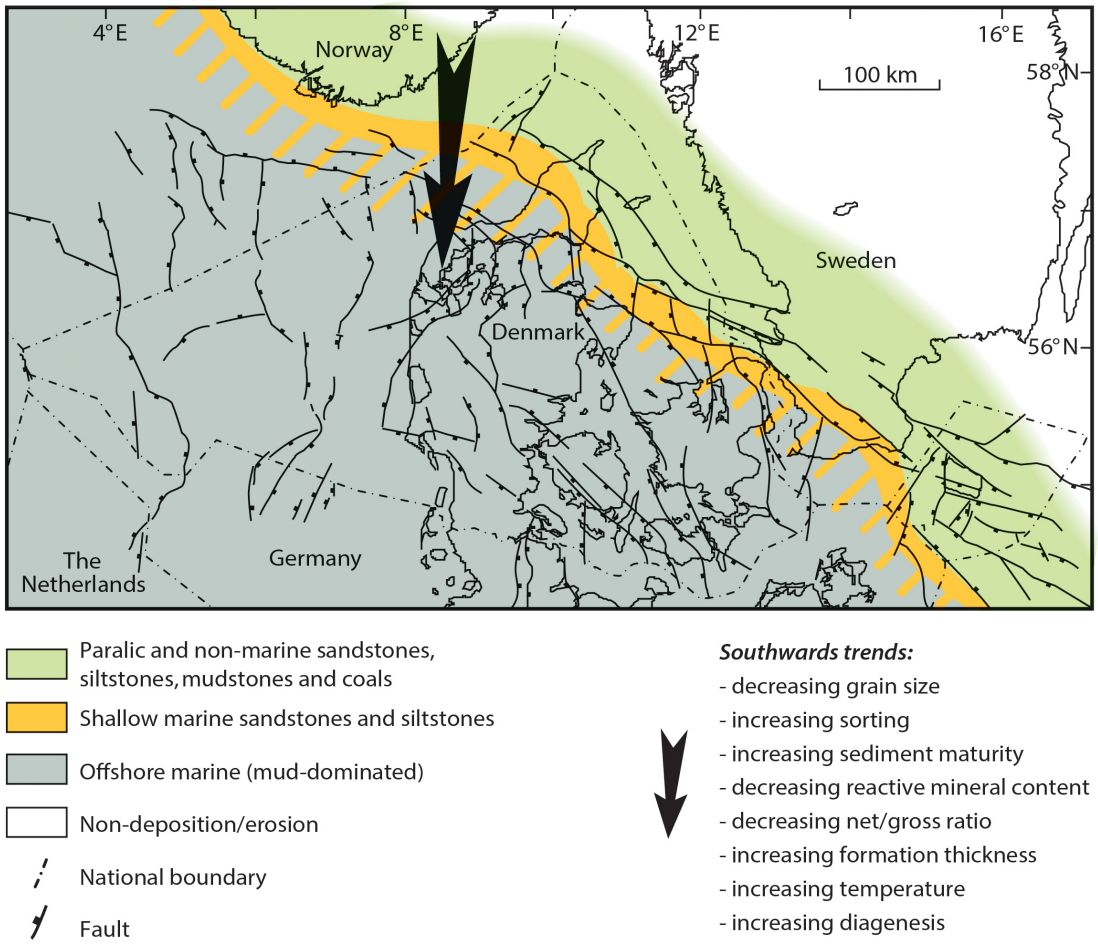

FIGURE 14 | Hettangian paleogeography from Michelsen et al. (2003) corresponding to the time when the upper part of the Gassum Formation was deposited. The facies belts shifted back and forth corresponding to repeated sea-level changes. The observed directional trends that influence the reservoir quality in the study area are listed.

storage volume within the formation increases in a northerly direction. However, the seismic interpretation shows that the total thickness of the formation decreases in the northernmost part of the study area (**Figures 2**, **3**). All these directional trends that affect the reservoir quality are summarized in **Figure 14** based on the results of this study compared to the findings of Weibel et al. (2017a,b). Comparable reactivity-related maturity trends of time-equivalent sediments deposited along the rim of the Fennoscandian Shield in the North Sea and Norwegian Sea may be assumed.

The sediments were only subjected to initial mesogenesis and a limited residence time at maximum burial before the Neogene inversion. Thus, the quartz overgrowths are thin and only minor amounts of authigenic clays were formed. The reservoir quality is therefore expected to be good in the Gassum Formation in the Skagerrak. Locally, pore-filling carbonate-cemented intervals occur in the onshore part of the formation, but they are mostly thin and associated with shell layers (Weibel et al., 2017a). The cemented interval observed in the 13/1-U-1 well is caused by abundant shell fragments, which are a result of the deposition as a transgressive lag. Observations from the more southern and eastern part of the formation show that pore-filling carbonate is most abundant in intervals of the shoreface and lagoonal depositional environments, but it also occurs in fluvial deposits (**Figure 13**; Weibel et al., 2017a,b). Only thin intervals of the sandstones are presumed to be pervasively carbonate cemented in the study area due to the limited mesogenesis that has affected the sandstones prior to structural inversion, especially in the northern part of the area, and the carbonate cement abundance probably decreases northwards since the formation most likely is more fluvially dominated toward the north (**Figure 7**).

Reservoir Characterization at CO_2 Injection Site

The tentative injection site considered here is located in the Sorgenfrei-Tornquist Zone in the southern part of the study area (**Figure 1**). This position secures a long possible migration path

within the inclined sandstone layers of the Gassum Formation. The potential injection site is located north of the F-1, K-1, Felicia-1, and J-1 wells and south of the 13/1-U-1 well. The net/gross ratio of 0.45–0.78 in the southern wells is likely to be higher at the injection site due to its location that is more proximal to the source area. The thickly developed succession in Felicia-1 constitutes an outlier in the central Skagerrak with its thickness of 260 m (**Table 1**). However, the seismic mapping shows that the Gassum Formation has large thicknesses of c. 100–150 centrally in the study area and is extra thick at the injection site due to faulting and therefore has the potential to store large amounts of CO_2 (**Figures 2**, **7**). The formation is here located at 1545–1675 ms TWT corresponding to about 1850–2130 m depth, indicating that the net sandstone thickness is in the order of 130–180 m and that the reservoir temperature is in the range of 60–80°C.

It is likely that fluvial sandstones are more abundant at the injection site than in the southern wells due to its more proximal position (**Figure 7**). This is supported by the findings of Nielsen (2003), who presented a detailed sequence stratigraphic interpretation onshore Denmark based on well logs and cores. Furthermore, in the study area, possible channel features are recognized along the base of (para)-sequences as troughs on seismic profiles (**Figure 5**). Inferred dominating channel orientation (i.e., north-south, semi-parallel with most lines), sand-sand contacts and low relief make quantification of channelization difficult. The transgressive succession in the 13/1-U-1 well shows that a marine incursion to the northern part of the study area occurred, as evident by the content of glauconite and chlorite ooids. The transgressive lag marks the end of sand deposition in this area due to the back-stepping coastline. This succession was probably deposited in an estuary where the fine-grained material was supplied by erosion of shoreface deposits and the coarser grains were transported by rivers from the north. The grains are characterized by large feldspars, plutonic rock fragments, quartz with undulatory extinction, polycrystalline quartz and quartz with rounded overgrowths, suggesting a combination of first and second cycle sand grains. The high amount of Fe-rich authigenic phases in the conglomerate, including chamosite, pyrite, siderite and pervasive ankerite, may have formed in response to the dissolution of mafic minerals, or they may have precipitated due to high supply of iron from rivers entering the sea similar to glauconite formation (Ehrenberg, 1993). The presence of rootlets in the sandstone below the conglomerate shows that subaerial exposure occurred at this time, which may explain dissolution of feldspar grains and kaolinite precipitation. Flooding of these subaerially exposed sediments by the generally fluctuating sea-level (Haq et al., 1988; Nielsen, 2003) resulted in reworking of large clasts, which occur in the conglomerate and also are found in small quantities in the very fine- to fine-grained sandstone with traces of glauconite.

The northwards on-lapping internal seismic reflectors at base of the Gassum Formation in the study area in combination with the identification of the Lower Sinemurian TS11 topping the formation in 13/1-U-1 and disappearing toward the south show that the Gassum Formation is younging toward the north (**Figures 2–4**, **7**). The general back-stepping of the basin margin that occurred during deposition of the upper part of the Gassum Formation (Nielsen, 2003) means that the shoreface belt and coastal plain moved northwards. Therefore, this was probably the prevalent mechanism of sandstone deposition in the upper part of the succession at the injection site, whereas fluvial sandstones presumably dominate in the lower part. Based on the grain sizes found in the sandstones, varying from mostly fine- to medium-grained onshore Denmark and in the distally located K-1 well to coarse-grained in the Felicia-1 well and medium- to very coarse-grained in the J-1 well, it is concluded that the grain size increases toward the north due to the shorter transport distance from the provenance. Thus, coarse-grained shoreface sandstones are estimated to be the predominant reservoir constituent at the injection site, and they are probably coarsening-upwards hence being medium-grained or perhaps fine-grained at their base. The well-log analysis is based on old logs, so it is possible that the porosities have been underestimated (**Table 1**) since larger porosities are indicated by the texture and grain size of the sandstones (**Figures 8–10**). Porosities of 22–28% and permeabilities of 200–600 mD are therefore suggested for the injection site when also taking the onshore equivalents into account (**Figure 13**).

Albite, oligoclase and chamosite are the most reactive mineral phases with respect to carbonatization of CO_2, so the amount, distribution and surface area of these minerals in the sandstones at the injection site are of importance. The average plagioclase content of c. 10 vol% in the Gassum Formation onshore western Denmark (Weibel et al., 2017a) is assumed to be higher in the Skagerrak due to the proximity to the source area. Hence, a total albite + oligoclase content of 15 wt.% is estimated for the injection site, which is in accordance with the abundance indicated by the element scans (**Figure 9**). Chamosite occurs as thick concentric coatings in abundant ooids, forming part of the conglomerate in the 13/1-U-1 well (**Figure 10D**), and as discontinuous coats on grains in both the sandstone and conglomerate. Small amounts of chlorite also occur in sandstones from the K-1 and J-1 wells. Patchy chlorite coatings are also present in some of the sandstones onshore Denmark and continuous chamosite coatings are ubiquitous in shoreface and estuarine-fluvial sandstones in a forced regressive systems tract in the upper part of the formation (Weibel et al., 2017a). This could be a regional phenomenon as the coatings are present in both of the two wells where this interval has been drilled. The reactive surface area of this grain-coating chamosite is considerably larger than the surface area of the feldspar grains.

Mineral CO_2 Sequestration Potential

To ensure supercritical conditions for CO_2 during injection, prospective reservoirs are located deeper than 800 m. A suitable injection area is indicated in **Figures 1**, **2**, where the top of Gassum Formation is at c. 1850 m depth. There are no lithological data from this area, and reservoir properties must be inferred from seismic interpretation and extrapolated from the nearest wells (i.e., 13/1-U-1, Felicia-1, J-1, and K-1).

Injected CO_2 will rise to the top of the reservoir and migrate up-dip toward the north, within a progradational para-sequence

capped by a transgressive surface and overlain by mudstones of the Fjerritslev Formation. According to the depositional model, a CO_2 plume will sweep through lower to upper shoreface deposits i.e., from fine- to medium-grained to coarse-grained sandstones. The most reactive phases in the observed mineral assemblages, with respect to carbonatization of CO_2, are albite, oligoclase and chamosite (Palandri and Kharaka, 2004). Trace minerals may also contribute cations to the solution, depending on reducing/oxidizing potential of injected fluids. Plagioclase contents are in the order of 6–15 wt.% (estimated from XRD data, **Supplementary Figure S2**, and SEM element scans, **Figure 9**) in porous samples representative of reservoir sandstone, of which oligoclase constitutes a minor fraction of assumed 3 wt.%, while most grains are albite. Chamosite (Fe-endmember of chlorite) contents are in the order of 1–2 wt.% (estimated from XRD). Total reaction potential with cations provided to solution by albite (Na), oligoclase (Ca, Na) and chamosite (Fe, minor Mg) were estimated for shoreface reservoir sandstone with 25% porosity (mass balance method described by Hellevang et al., 2013). Comparing more reactive sediment (12 wt.% albite, 3 wt.% oligoclase and 2 wt.% chamosite) with a less reactive case (6 wt.% albite, 0 wt.% oligoclase and 1 wt.% chamosite), the total carbonatization potential for CO_2 precipitated as siderite, calcite and dawsonite ranges between 2.28 and 5.29 mol/L formation water. Disregarding dawsonite (as its relevance is somewhat disputed, e.g., Hellevang et al., 2005), the mineralization potential would be between 0.47 and 1.1 mol/L.

High salinities, in the order of 100–200 g/l, are reported for formation water in the Gassum Formation in the Danish Basin (Laier, 2008; Holmslykke et al., 2019). However, the data and established salinity-depth correlations may not be representative for the suggested injection site. The reported water chemistries are affected by deeper burial and proximity to thick, underlying Zechstein salt deposits, as well as super-saline Triassic porewaters. There are no formation water data from the 13/1-U-1 well, which would be most representative for the suggested injection site. It is likely that formation waters in the injection area are much less saline, given the nearshore location, the longer distance to salt deposits and the structural setting with a landwards slope. CO_2 experiments with sandstones from the Gassum Formation from central parts of the basin have shown small reaction potential during the experiment period (Weibel et al., 2014). However, the higher feldspar and chlorite contents and presumed less saline brines at the basin margin makes this area more prospective regarding carbonatization potential. Given relatively warm reservoir conditions ($>80°C$), the mineralization potential in a time frame of some hundred years is likely to be relevant (>5.5 kg CO_2 per m^3 reservoir), although not very high. Immobilization of CO_2 by dissolution and mineralization may also be optimized with respect to spreading in different sedimentary facies settings by means of adapted injection strategies (Sundal et al., 2015).

The content of reactive phases is higher in less mature sediment, as plagioclase is more intact. Also, in sediment derived from the Telemarkia Terrane, metamorphic rocks of greenschist facies in southern regions are likely to contribute with more chlorite and albite compared to sediments from the Idefjorden Terrane. Thus, the total mineral reaction potential, although probably moderate, increases toward the top of the reservoir and toward more proximal parts in the study area. Varying grain size in different sedimentary facies and heterogeneity will also affect the reactive contact areas and overall mineralization potential. Generally, there are good prospects for migration-assisted storage in the Gassum Formation. The reservoir properties are presumably ideal, allowing for effective injection and for CO_2 to migrate upslope, becoming immobilized through structural, residual and dissolution trapping, while an open boundary allows for efficient pressure dissipation.

There is a general lack of data, which is the main challenge in this area and in many other prospective CO_2 reservoirs, as data collection from uneconomical saline aquifers is rather limited. Hence, it is important to utilize regional knowledge to delineate relevant trends both in a traditional sense for reservoir properties and also with respect to reactivity. As provenance shifts with time and causes a more reactive mineral assembly, it is inferred to change upwards in the studied succession. The major novelty of the approach is to use provenance analysis to help determining the reactivity of the reservoir rocks, which has not been considered before although this can provide important information. Also, the extrapolation of facies belts and evaluation of the effect of burial diagenesis on reservoir properties is new for this part of the basin, and a valuable addition to the overall estimation of storage potential available to Europe.

CONCLUSION

Sedimentary facies and mineral assemblages provide constraints on the reaction potential for CO_2 in the Gassum Formation. Detailed delineation of stratigraphic surfaces and evaluation of sediment provenance have not previously been presented for this area. Linking reactivity to provenance and sediment maturity proved to be a useful tool to point out immobilization potentials in different parts of the reservoir. Corresponding basinward maturity trends are presumed to be present along the rim of the Fennoscandian Shield in the North Sea and Norwegian Sea.

The source area extent decreases with time through the succession, providing more reactive minerals and sediment with higher potential for mineralization of CO_2 in the top part of the reservoir. CO_2 is buoyant and will rise upwards, meaning that CO_2 migration will occur mostly in lower to upper shoreface facies within relatively immature, fine- to coarse-grained sand of increasing reactivity up depositional dip (closer to source areas). Temperature and reaction kinetics will decrease in shallower parts, however, and the total mineralization potential is moderate (>5.5 kg CO_2 per m^3).

The largest provenance area with zircons supplied from seven different basement terranes in the Fennoscandian Shield is found in the sample with the most mature mineralogy, reflecting the longer transport distance during this estuarine lowstand setting, which may partly be related to recycling of sediments. The highstand setting of the shoreface sandstones has resulted in immature mineralogy due to predominant sediment transport from the adjacent Telemarkia Terrane. The most reactive

phases with regards to mineral sequestration of CO_2 comprise albite, oligoclase and chlorite. The feldspar content decreases southwards due to mechanical breakdown and weathering, whereas chlorite coatings and ooids are most abundant in the northern and upper part of the formation, presumably because they are sourced by alteration of unstable heavy minerals or by iron from rivers. Provenance including mineralogy and transport distance exerts a stronger influence on total reactivity than the sedimentary facies setting (fluvial vs. shoreface).

Based on observed diagenetic alterations, the maximum burial depths prior to structural inversion are estimated to be within 2.3–3.0 km. Thus, burial diagenesis has not reduced the reservoir quality drastically. Pore-filling carbonate cementations occur only locally. From the proposed injection area, CO_2 would move into progressively more mineralogically immature sediments with presumed excellent reservoir quality.

DATA AVAILABILITY STATEMENT

All datasets generated for this study are included in the article/**Supplementary Material**.

AUTHOR CONTRIBUTIONS

MO and AS wrote the manuscript with support from the other authors. MO, AS, and RW did the petrographic work. UG and IB performed the seismic interpretation. TT was in charge of the zircon age analyses. MO made the provenance interpretation. LK did the well-log interpretation. AS and HH made the reactivity estimates. LN performed the sedimentological work.

FUNDING

This contribution is part of the CO_2-Upslope project that is funded by CLIMIT and the Research Council of Norway under grant #268512.

ACKNOWLEDGMENTS

We would like to acknowledge NPD, Sintef and Atle Mørk for access to the 13/1-U-1 core, and GEUS for providing samples from K-1, J-1 and Felicia-1. Thanks to B. G. Haile, T. Naidoo, S. Simonsen, M. Heeremans, L. H. Line and S. Akhavan at the Department of Geosciences at UiO and S. H. Serre, M. Alaei, M. Leth, J. L. Bendtsen, and J. Halskov at GEUS for technical assistance and discussions. The reviewers and editor are thanked for valuable advice that helped improve the manuscript.

SUPPLEMENTARY MATERIAL

The Supplementary Material for this article can be found online at: https://www.frontiersin.org/articles/10.3389/feart.2019.00312/full#supplementary-material

FIGURE S1 | Cathodoluminescence photo of detrital zircon grains from the Gassum Formation used for U-Pb age dating.

FIGURE S2 | X-ray diffraction results of samples from the Gassum Formation in the Skagerrak.

TABLE S1 | Zircon U-Pb age data from the Gassum Formation in the Skagerrak.

REFERENCES

Aagaard, P., Egeberg, P. K., Saigal, G. C., Morad, S., and Bjørlykke, K. (1990). Diagenetic albitization of detrital K-feldspars in jurassic, lower cretaceous and tertiary clastic reservoir rocks from offshore Norway, II. Formation water chemistry and kinetic considerations. *J. Sediment. Petrol.* 60, 575–581. doi: 10.1306/212f91ec-2b24-11d7-8648000102c1865d

Åhäll, K. I., Cornell, D. H., and Armstrong, R. (1998). Ion probe zircon dating of metasedimentary units across the Skagerrak: new constraints for early mesoproterozoic growth of the Baltic Shield. *Precambrian Res.* 87, 117–134. doi: 10.1016/s0301-9268(97)00059-4

Andersen, T., Griffin, W. L., and Sylvester, A. G. (2007). Sveconorwegian crustal underplating in southwestern Fennoscandia: LAM-ICPMS U-Pb and Lu-Hf isotope evidence from granites and gneisses in Telemark, southern Norway. *Lithos* 93, 273–287. doi: 10.1016/j.lithos.2006.03.068

Anthonsen, K. L., Aagaard, P., Bergmo, P. E. S., Gislason, S. R., Lothe, A. E., Mortensen, G. M., et al. (2014). Characterisation and selection of the most prospective CO2 storage sites in the Nordic region. *Energy Procedia* 63, 4884–4896. doi: 10.1016/j.egypro.2014.11.519

Baig, I., Faleide, J. I., Mondol, N. H., and Jahren, J. (2019). Burial and exhumation history controls on shale compaction and thermal maturity along the Norwegian North Sea basin margin areas. *Mar. Pet. Geol.* 104, 61–85. doi: 10.1016/j.marpetgeo.2019.03.010

Bergmo, P. E. S., Polak, S., Aagaard, P., Frykman, P., Haugen, H. A., and Bjørnsen, D. (2013). Evaluation of CO2 storage potential in skagerrak. *Energy Procedia* 37, 4863–4871. doi: 10.1016/j.egypro.2013.06.396

Bertelsen, F. (1978). The upper triassic – lower jurassic vinding and gassum formations of the Norwegian-Danish Basin. *Geol. Surv. Denmark Ser. B* 3:26.

Bertelsen, F. (1980). Lithostratigraphy and depositional history of the Danish Triassic. *Geol. Surv. Denmark Ser. B* 4:59.

Bingen, B., Nordgulen, Ø, and Viola, G. (2008). A four-phase model for the sveconorwegian orogeny, SW Scandinavia. *Nor. J. Geol.* 88, 43–72.

Bingen, B., Skår, Ø, Marker, M., Sigmond, E. M. O., Nordgulen, Ø, Ragnhildstveit, J., et al. (2005). Timing of continental building in the sveconorwegian orogen, SW Scandinavia. *Nor. J. Geol.* 85, 87–116.

Bingen, B., and Solli, A. (2009). Geochronology of magmatism in the caledonian and sveconorwegian belts of Baltica: synopsis for detrital zircon provenance studies. *Norw. J. Geol.* 89, 267–290.

Bjørlykke, K. (1998). Clay mineral diagenesis in sedimentary basins – a key to the prediction of rock properties. Examples from the North Sea Basin. *Clay Minerals* 33, 15–34. doi: 10.1180/claymin.1998.033.1.03

Bjørlykke, K., Aagaard, P., Dypvik, H., Hastings, D. S., and Harper, A. S. (1986). "Diagenesis and reservoir properties of jurassic sandstones from the hahenbanken area, offshore mid Norway," in *Habitat of hydrocarbons on the Norwegian continental shelf*, ed. A. M. Spencer, (London: Graham & Trotman Ltd.), 275–286.

Bjørlykke, K., Jahren, J., Mondol, N. H., Marcussen, Ø, Croize, D., Peltonen, C., et al. (2009). Sediment compaction and rock properties. *Search Discov. Article* 50192, 1–8.

Brewer, T. S., Daly, J. S., and Åhall, K.-I. (1998). Contrasting magmatic arcs in the palaeoproterozoic of the south-western Baltic Shield. *Precambrian Res.* 92, 297–315. doi: 10.1016/s0301-9268(98)00079-5

Burley, S. D., Mullis, J., and Matter, A. (1989). Timing diagenesis in the tartan reservoir (UK North Sea): constraints from combined cathodoluminescence microscopy and fluid inclusion studies. *Mar. Pet. Geol.* 6, 98–120. doi: 10.1016/0264-8172(89)90014-7

Corfu, F., Larsen, B. T., and Ganerød, M. (2015). "Geochronology of Krogskogen rombporphyry lavas by U-Pb and Ar-Ar and relations to Oslo Rift chronology," in *31st Geological Winter Meeting, Abstracts and Proceedings of the Geological Society of Norway*, (Stavanger).

Ehrenberg, S. N. (1993). Preservation of anomalously high porosity in deeply buried sandstones by grain-coating chlorite: examples from the Norwegian continental shelf. *Am. Assoc. of Pet. Geol. Bull.* 77, 1260–1286.

Eiken, O., Ringrose, P., Hermanrud, C., Nazarian, B., Torp, T. A., and Høier, L. (2011). Lessons learned from 14 years of CCS operations: sleipner. In salah and snøhvit. *Energy Procedia* 4, 5541–5548. doi: 10.1016/j.egypro.2011.02.541

Erlström, M., and Sivhed, U. (2012). Pre-Rhaetian Triassic strata in Scania and adjacent offshore areas –stratigraphy, petrology and subsurface characteristics. *Geological Survey of Sweden Rapporter och meddelanden* 132:74.

Fisher, R. S., and Land, L. S. (1986). Diagenetic history of eocene wilcox sandstones, South-Central Texas. *Geochim. t Cosmochim. Acta* 50, 551–561. doi: 10.1016/0016-7037(86)90104-3

Folk, R. L. (1966). A review of grain-size parameters. *Sedimentology* 6, 73–93. doi: 10.1111/j.1365-3091.1966.tb01572.x

Garzanti, E., Andò, S., and Vezzoli, G. (2008). Settling equivalence of detrital minerals and grain-size dependence of sediment composition. *Earth Planet. Sci. Lett.* 273, 138–151. doi: 10.1016/j.epsl.2008.06.020

Halland, E. K., Gjeldvik, I. T., Johansen, W. T., Magnus, C., Meling, I. M., Pedersen, S., et al. (2011). *CO2 storage atlas Norwegian North Sea*. Stavanger: Norwegian Petroleum Directorate, 163.

Hamberg, L., and Nielsen, L. H. (2000). Shingled, sharp-based shoreface sandstones: depositional response to stepwise forced regression in a shallow basin, upper triassic gassum formation, denmark. *Geol. Soc. Lon. Spec. Publications* 172, 69–89. doi: 10.1144/gsl.sp.2000.172.01.04

Haq, B. U., Hardenbol, J., and Vail, P. R. (1988). "Mesozoic and Cenozoic chronostratigraphy and cycles of sea-level change," in *Sea Level Changes: An Integrated Approach*, ed. C. K. Wilgus, (Houston: SEPM Special Publication).

Heeremans, M., and Faleide, J. I. (2004). Late Carboniferous-Permian tectonics and magmatic activity in the Skagerrak, Kattegat and the North Sea. *Geol. Soc. Lon. Spec. Publications* 223, 157–176. doi: 10.1144/gsl.sp.2004.223.01.07

Hellevang, H., Aagaard, P., Oelkers, E. H., and Kvamme, B. (2005). Can dawsonite permanently trap CO2? *Environ. Sci. Technol.* 39, 8281–8287. doi: 10.1021/es0504791

Hellevang, H., Pham, V. T. H., and Aagaard, P. (2013). Kinetic modelling of CO2–water–rock interactions. *Int. J. Greenhouse Gas Control* 15, 3–15. doi: 10.1016/j.ijggc.2013.01.027

Hellström, J., Paton, C., Woodhead, J., and Hergt, J. (2008). "Iolite: Software for spatially resolved LA- (quad and MC) ICPMS analysis," in *Laser Ablation ICP–MS in the Earth Sciences: Current Practices and Outstanding Issues. Mineral*, ed. P. Sylvester, (Quebec: Assoc. of Canada), 343–348.

Hervig, R. L., Williams, L. B., Kirkland, I. K., and Longstaffe, L. J. (1995). Oxygen isotope microanalyses of diagenetic quartz: possible low temperature occlusion of pores. *Geochim. Cosmochim. Acta* 59, 2537–2543. doi: 10.1016/0016-7037(95)00148-4

Holmslykke, H. D., Schovsbo, N. H., Kristensen, L., Weibel, R., and Nielsen, L. H. (2019). Characterising brines in deep Mesozoic sandstone reservoirs, Denmark. *Geol. Surv. Denmark Greenland Bull.* 43:e2019430104.

Jackson, S. E., Pearson, N. J., Griffin, W. L., and Belousova, E. A. (2004). The application of laser ablation-inductively coupled plasma-mass spectrometry to in situ U–Pb zircon geochronology. *Chem. Geol.* 211, 47–69. doi: 10.1016/j.chemgeo.2004.06.017

Japsen, P., and Bidstrup, T. (1999). Quantification of late Cenozoic erosion in Denmark based on sonic data and basin modelling. *Bull. Geol. Soc. Denmark* 46, 79–99.

Japsen, P., Green, P. F., Bonow, J. M., and Erlström, M. (2016). Episodic burial and exhumation of the southern baltic shield: epeirogenic uplifts during and after break-up of Pangaea. *Gondwana Res.* 35, 357–377. doi: 10.1016/j.gr.2015.06.005

Japsen, P., Green, P. F., Nielsen, L. H., Rasmussen, E. S., and Bidstrup, T. (2007). Mesozoic-cenozoic exhumation events in the eastern North Sea Basin: a multi-disciplinary study based on palaeothermal, palaeoburial, stratigraphic and seismic data. *Basin Res.* 19, 451–490. doi: 10.1111/j.1365-2117.2007.00329.x

Jarsve, E. M., Maast, T. E., Gabrielsen, R. H., Faleide, J. I., Nystuen, J. P., and Sassier, C. (2014). Seismic stratigraphic subdivision of the triassic succession in the Central North Sea; integrating seismic reflection and well data. *J. Geol. Soc.* 171, 353–374. doi: 10.1144/jgs2013-056

Kristensen, L., Hjuler, M. L., Frykman, P., Olivarius, M., Weibel, R., Nielsen, L. H., et al. (2016). Pre-drilling assessments of average porosity and permeability in the geothermal reservoirs of the Danish area. *Geothermal Energy* 4, 1–27.

Lahtinen, R., Garde, A. A., and Melezhik, V. A. (2008). Paleoproterozoic evolution of Fennoscandia and Greenland. *Episodes* 31, 20–28. doi: 10.18814/epiiugs/2008/v31i1/004

Laier, T. (2008). *Chemistry of Danish saline formation waters relevant for core fluid experiments. Fluid chemistry data for lab experiments related to CO2 storage in deep aquifers. Geological Survey of Denmark and Greenland*. Report 2008/48. Karbunya St: GEUS

Larsen, G. (1966). Rhaetic-Jurassic-Lower Cretaceous sediments in the Danish Embayment. *A heavy-mineral study. Geol. Surv. Denmark Ser.* 2:127.

Lindström, S., Vosgerau, H., Piasecki, S., Nielsen, L. H., Dybkjær, K., and Erlström, M. (2009). Ladinian palynofloras in the Norwegian–Danish Basin: a regional marker reflecting a climate change. *Geol. Surv. Denmark Greenland Bull.* 17, 21–24.

Malusà, M. G., Resentini, A., and Garzanti, E. (2016). Hydraulic sorting and mineral fertility bias in detrital geochronology. *Gondwana Res.* 31, 1–19. doi: 10.1016/j.gr.2015.09.002

Metz, B., Davidson, O., De Coninck, H., Loos, M., and Meyer, L. (2005). *Carbon dioxide capture and storage. IPCC Special Report*. Geneva: IPCC, 431.

Michelsen, O. (1975). Lower jurassic biostratigraphy and ostracods of the danish embayment. *Geol. Surv. Denmark II Række Ser.* 104:287.

Michelsen, O. (1978). Stratigraphy and distribution of Jurassic deposits of the Norwegian–Danish Basin. *Geol. Sur. Denmark Ser. B* 2:28.

Michelsen, O., and Clausen, O. R. (2002). Detailed stratigraphic subdivision and regional correlation of the southern Danish Triassic succession. *Mar. Pet. Geol.* 19, 563–587. doi: 10.1016/s0264-8172(02)00028-4

Michelsen, O., Nielsen, L. H., Johannessen, P. N., Andsbjerg, J., and Surlyk, F. (2003). Jurassic lithostratigraphy and stratigraphic development onshore and offshore Denmark. *Geol. Sur. Denmark Greenland Bull.* 1, 147–216.

Morad, S. (1990). Mica alteration reactions in Jurassic reservoir sandstones from the Haltenbanken area, offshore Norway. *Clays Clay Minerals* 38, 584–590. doi: 10.1346/ccmn.1990.0380603

Nielsen, L. H. (2003). Late triassic – jurassic development of the danish basin and the fennoscandian Border Zone, southern scandinavia. *Geol. Surv. Denmark Greenland Bull.* 1, 459–526.

Nielsen, L. H., and Japsen, P. (1991). Deep wells in Denmark 1935–1990. lithostratigraphic subdivision. *Geol. Surv. Denmark Ser. A* 31:178.

Olivarius, M., and Nielsen, L. H. (2016). Triassic paleogeography of the greater eastern Norwegian-Danish Basin: constraints from provenance analysis of the Skagerrak Formation. *Mar. Pet. Geol.* 69, 168–182. doi: 10.1016/j.marpetgeo.2015.10.008

Olivarius, M., Rasmussen, E. S., Siersma, V., Knudsen, C., Kokfelt, T. F., and Keulen, N. (2014). Provenance signal variations caused by facies and tectonics: zircon age and heavy mineral evidence from miocene sand in the north-eastern North Sea Basin. *Mar. Pet. Geol.* 49, 1–14. doi: 10.1016/j.marpetgeo.2013.09.010

Olivarius, M., Weibel, R., Friis, H., Boldreel, L. O., Keulen, N., and Thomsen, T. B. (2017). Provenance of the Lower Triassic Bunter Sandstone Formation: implications for distribution and architecture of aeolian vs. fluvial reservoirs in the North German Basin. *Basin Res.* 29(Suppl. 1), 113–130. doi: 10.1111/bre.12140

Palandri, J. L., and Kharaka, Y. K. (2004). *A Compilation of Rate Parameters of Water-Mineral Interaction Kinetics for Application to Geochemical Modeling (No. OPEN-FILE-2004-1068)*. Menlo Park CA.: Geological Survey.

Paton, C., Hellstrom, J. C., Paul, P., Woodhead, J. D., and Hergt, J. M. (2011). Iolite: freeware for the visualisation and processing of mass spectrometric data. *J. Anal. Atomic Spectrometry* 26, 2508–2518.

Petrus, J. A., and Kamber, B. S. (2012). VizualAge: a novel approach to laser ablation ICP-MS U-Pb geochronology data reduction. *Geostand. Geoanal. Res.* 36, 247–270. doi: 10.1111/j.1751-908x.2012.00158.x

Rohrman, M., van der Beek, P., Andriessen, P., and Cloeting, S. (1995). Meso-Cenozoic morphotectonic evolution of southern Norway: neogene domal uplift

inferred from apatite fission track thermochronology. *Tectonics* 14, 704–718. doi: 10.1029/95tc00088

Saigal, G. C., Morad, S., Bjørlykke, K., Egeberg, P. K., and Aagaard, P. (1988). Diagenetic albitization of detrital K-feldspar in Jurassic. *J. Sediment. Petrol.* 58, 1003–1013.

Schmidt, B. J. (1985). Clay mineral investigation of the rhaetic-jurassic-lower cretaceous sediments of the Børglum 1 and Uglev 1 wells. *Denmark. Bull. Geol. Soc. Denmark* 34, 97–110.

Slama, J. (2016). Rare late neoproterozoic detritus in SW Scandinavia as a response to distant tectonic processes. *Terra Nova* 28, 394–401. doi: 10.1111/ter.12232

Slama, J., Kosler, J., Condon, D. J., Crowley, J. L., Gerdes, A., Hanchar, J. M., et al. (2008). Plesovice zircon - a new natural reference material for U-Pb and Hf isotopic microanalysis. *Chem. Geol.* 249, 1–35. doi: 10.1016/j.chemgeo.2007.11.005

Smelror, M., Jacobsen, T., Rokoengen, K., Bakke, S., Bø, R., Goll, R. M., et al. (1989). *Shallow Drilling Farsund Subbasin: Main Report. IKU report 21*. Trondheim: Institute for Continental Shelf Research.

Sundal, A., Miri, R., Ravn, T., and Aagaard, P. (2015). Modelling CO2 migration in aquifers; considering 3D seismic property data and the effect of site-typical depositional heterogeneities. *Int. J. Greenhouse Gas Control* 39, 349–365.

Thomsen, T. B., Heijboer, T., and Guarnieri, P. (2016). jAgeDisplay: software for evaluation of data distributions in U-Th-Pb geochronology. *Geol. Surv. Denmark Greenland Bull.* 35, 103–106.

Troedsson, G. (1951). *On the Höganäs series of Sweden (Rhaeto-Lias)*. Lund: C.W.K. Gleerup, 268.

Upslope (2019). Optimized CO2 Storage in Sloping Aquifers. The CO2-Upslope Project is Funded by the CLIMIT-Programme, Grant Number 268512. Available at: www.mn.uio.no/geo/english/research/projects/upslope (accessed November 15, 2019).

Van Wagoner, J. C., Mitchum, R. M., Campion, K. M., and Rahmanian, V. D. (1990). Siliciclastic sequence stratigraphy in well logs, cores, and outcrops: concepts for high-resolution correlation of time and facies. *Am. Assoc. Pet. Geol. Methods Explor. Ser.* 7:55. doi: 10.1306/Mth7510

Vejbæk, O. V., and Britze, P. (1994). *Geological Map of Denmark 1:750.000. Top pre-Zechstein (two-way traveltime and depth)*. Map Series 45. Copenhagen: Geological Survey of Denmark, 8.

Weibel, R., Friis, H., Kazerouni, A. M., Svendsen, J. B., Stokkendal, J., and Poulsen, M. L. K. (2010). Development of early diagenetic silica and quartz morphologies – Examples from the Siri Canyon. Danish North Sea. *Sediment. Geol.* 228, 151–170. doi: 10.1016/j.sedgeo.2010.04.008

Weibel, R., Kjøller, C., Bateman, K., Laier, T., Nielsen, L. H., and Purser, G. (2014). Carbonate dissolution in mesozoic sand- and claystones as a response to CO2 exposure at 70°C and 20 MPa. *Appl. Geochem.* 42, 1–15. doi: 10.1016/j.apgeochem.2013.12.006

Weibel, R., Olivarius, M., Kristensen, L., Friis, H., Hjuler, M. L., Kjøller, C., et al. (2017a). Predicting permeability of low-enthalpy geothermal reservoirs: a case study from the upper triassic - lower jurassic gassum formation. Norwegian–Danish Basin. *Geothermics* 65, 135–157. doi: 10.1016/j.geothermics.2016.09.003

Weibel, R., Olivarius, M., Kjøller, C., Kristensen, L., Hjuler, M. L., Friis, H., et al. (2017b). The influence of climate on early and burial diagenesis of Triassic and Jurassic sandstones from the Norwegian–Danish Basin. *Depos. Rec.* 3, 60–91. doi: 10.1002/dep2.27

Wentworth, C. K. (1922). A scale of grade and class terms for clastic sediments. *J. Geol.* 30, 377–392. doi: 10.1086/622910

Wiedenbeck, M., Allé, P., Corfu, F., Griffin, W. L., Meier, M., Oberli, F., et al. (1995). Three natural zircon standards for U-Th-Pb, Lu-Hf, trace element and REE analyses. *Geostand. Newslett.* 19, 1–23. doi: 10.1111/j.1751-908x.1995.tb00147.x

Wiedenbeck, M., Hanchar, J. M., Peck, W. H., Sylvester, P., Valley, J., Whitehouse, M., et al. (2004). Further characterisation of the 91500 zircon crystal. *Geostand. Geoanal. Res.* 28, 9–39. doi: 10.1111/j.1751-908x.2004.tb01041.x

Conflict of Interest: The authors declare that the research was conducted in the absence of any commercial or financial relationships that could be construed as a potential conflict of interest.

Copyright © 2019 Olivarius, Sundal, Weibel, Gregersen, Baig, Thomsen, Kristensen, Hellevang and Nielsen. This is an open-access article distributed under the terms of the Creative Commons Attribution License (CC BY). The use, distribution or reproduction in other forums is permitted, provided the original author(s) and the copyright owner(s) are credited and that the original publication in this journal is cited, in accordance with accepted academic practice. No use, distribution or reproduction is permitted which does not comply with these terms.